EUROPEAN RESPIRATORY journal
FLAGSHIP SCIENTIFIC JOURNAL OF ERS

Early View

Original research article

Targeting peptidyl-prolyl isomerase 1 in experimental pulmonary arterial hypertension

Nabham Rai, Akylbek Sydykov, Baktybek Kojonazarov, Jochen Wilhelm, Grégoire Manaud, Swathi Veeroju, Clemens Ruppert, Frédéric Perros, Hossein Ardeschir Ghofrani, Norbert Weissmann, Werner Seeger, Ralph T. Schermuly, Tatyana Novoyatleva

Please cite this article as: Rai N, Sydykov A, Kojonazarov B, *et al*. Targeting peptidyl-prolyl isomerase 1 in experimental pulmonary arterial hypertension. *Eur Respir J* 2022; in press (https://doi.org/10.1183/13993003.01698-2021).

Targeting peptidyl-prolyl isomerase 1 in experimental pulmonary arterial hypertension

Nabham Rai[1], Akylbek Sydykov[1], Baktybek Kojonazarov[1,2], Jochen Wilhelm[1,2], Grégoire Manaud[3], Swathi Veeroju[1], Clemens Ruppert[2], Frédéric Perros[3], Hossein Ardeschir Ghofrani[1], Norbert Weissmann[1], Werner Seeger[1,2,4], Ralph T. Schermuly[1]* and Tatyana Novoyatleva[1]*

Short title: Rai N. – Pin1 in experimental PAH

Affiliations:

[1]*Universities of Giessen and Marburg Lung Center (UGMLC), Excellence Cluster Cardio Pulmonary Institute (CPI), Member of the German Center for Lung Research (DZL), Justus-Liebig-University Giessen, Giessen, Germany (N.R., A.S., B.K., J.W., S.V., C. R., N.W., H.A.G., W.S., T.N, R.T.S.)*

[2]*Institute for Lung Health*

[3]*Université Paris–Saclay, AP-HP, INSERM UMR_S 999, Service de Pneumologie et Soins Intensifs Respiratoires, Hôpital de Bicêtre, Le Kremlin Bicêtre, France (G.M, F.R).*

[4]*Max Planck Institute for Heart and Lung Research, Bad Nauheim, Germany (W.S.)*

**These co-senior authors contributed equally to this work*

Correspondence to: *Tatyana Novoyatleva, Ph.D. Department of Pulmonary Pharmacotherapy, Justus-Liebig-University Giessen, Aulweg 130, 35392 Giessen, Germany. E-mail tayana.novoyatleva@innere.med.uni-giessen.de*

Total word count: 5021 words (3386 in main text)

Abstract

Pulmonary arterial hypertension (PAH) is a progressive disease characterized by pro-proliferative and anti-apoptotic phenotype in vascular cells, leading to pulmonary vascular remodeling and right heart failure. Peptidylprolyl cis/trans isomerase, NIMA interacting 1 (Pin1), a highly conserved enzyme, which binds to and catalyzes the isomerization of specific phosphorylated Ser/Thr-Pro motifs, acting as a molecular switch in multiple coordinated cellular processes. We hypothesized that Pin1 plays a substantial role in PAH and its inhibition with a natural organic compound, Juglone, would reverse experimental pulmonary hypertension (PH).

We demonstrated that the expression of Pin1 was markedly elevated in experimental PH (i.e. hypoxia induced mouse and Sugen/hypoxia induced rat models) and pulmonary arterial smooth muscle cells (PASMCs) of patients with clinical PAH. *In vitro* Pin1 inhibition by either Juglone treatment or siRNA knock-down resulted in an induction of apoptosis and decrease in proliferation of human pulmonary vascular cells. Stimulation with growth factors induced Pin1 expression, while its inhibition reduced the activity of numerous PAH-related transcription factors, such as hypoxia-inducible factor alpha (HIF) and signal transducer and activator of transcription (STAT). Juglone administration lowered pulmonary vascular resistance, enhanced RV function, improved pulmonary vascular and cardiac remodeling in the Sugen/hypoxia rat model of PAH and the chronic hypoxia-induced PH model in mice.

Our study demonstrates that targeting of Pin1 with small molecule inhibitor, Juglone, might be an attractive future therapeutic strategy for PAH and right heart disease secondary to PAH.

Introduction

Pulmonary arterial hypertension (PAH) is a fatal pulmonary vascular disease characterized by pulmonary vascular remodeling and increased pulmonary vascular resistance, culminating in right ventricular (RV) hypertrophy and failure [1]. The dynamic vasoconstriction of pulmonary arteries, their adverse structural remodeling, fibrosis and stiffening, are the main causes of increased pulmonary vascular resistance [2]. PAH shares some common features with cancer, as the increase in cell proliferation and resistance to apoptosis [3]. Besides this, endothelial dysfunction, an increase in inflammation, dysregulated angiogenesis, metabolic disturbance, oxidative stress and mitochondrial dysregulation contribute to the progression of the disease [4]. PAH is a complex and multifactorial disease, which emergence has been explained by a concept known as the “multiple-hit hypothesis”, in which combination of two or more hits is essential for triggering of key mechanisms that lead to vascular constriction [5-7].

The peptidyl-prolyl cis**/**trans isomerase (Pin1), is a highly conserved enzyme, which belongs to the PPI-ase superfamily of proteins, comprising of cyclophilins, FK506-binding proteins (FKBPs), and parvulins [8]. Pin1 is the only known PPIase, which specifically and uniquely recognizes phosphorylated Ser/Thr-Pro peptides and catalyzes the cis**/**trans isomerization of these pSer/Thr-Pro motifs [9, 10]. Post-phosphorylation cis**/**trans isomerization, driven by Pin1 induces structural changes further affecting phosphorylation/dephosphorylation status of target proteins [11-14]. As a consequence, conformational modifications of many target phosphoproteins affect their stability and activity, subcellular localization and protein-protein interactions (PTMs), triggering multiple cellular signaling pathways [14-16]. Thus, Pin1 serves as a molecular determinant of the fate of phosphoproteins [14], which adds a new layer of control in various signaling pathways [17]. Amongst Pin1 substrates are numerous cell cycle-regulatory proteins, as cell division cycle 25 (Cdc25) [18], Cyclin D1 [19, 20], Cyclin E [21], Polo-like kinase 1 (Plk1) [22, 23]; transcription factors, as Retinoblastoma protein (Rb) [24], neurogenic locus notch homolog protein 1 (Notch1) [24], DNA-damage factors, as CREB-binding protein/p300 (CBP/p300) [25], homeodomain-interacting protein kinase 2 (HIPK2) and apoptotic regulatory proteins, as tumor suppressor p53 [26, 27], and survivin [28]. In association with this number of various signaling pathways, including cell

cycle progression, gene transcription, tumor development, oxidative stress and apoptosis are markedly affected by Pin1 [17], thus regulation driven by Pin1 provides a new platform for assembly of multiple protein networks.

Here we investigated the expression and the role of Pin1 in experimental and clinical PAH by using Juglone, a specific and irreversible Pin1 inhibitor, established to covalently inactivate Pin1 [29, 30]**.** We show that inhibition of Pin1 by the Juglone efficiently ameliorated both hypoxia (chronic hypoxia mouse model) and non-hypoxia (Sugen5416 combined with chronic hypoxia rat model) induced PAH.

Overall, our data indicate that Juglone provides beneficial outcomes on RV hypertrophy, RV systolic pressure and RV function in both hypoxia and non-hypoxia induced experimental PH, suggesting that targeting of Pin1 activity offers a potential therapeutic option for PH.

Methods

Animals

All *in vivo* procedures were approved by local and federal Animal Ethics Committee Authorities (approval number: GI 20/10 Nr. G 82/2018).

Cell culture and reagents

Human pulmonary artery smooth muscle cells (hPASMCs) were either obtained from the UGMLC Giessen Biobank, member of the DZL Platform Biobanking or purchased from Lonza (Basel, Switzerland). Murine PASMCs were isolated directly from precapillary pulmonary arterial vessels using iron particles, as previously described [31, 32]. Human pulmonary artery endothelial cells (hPAECs) from healthy individuals were purchased from Lonza (Basel, Switzerland). IPAH hPAECs were produced as previously described [33]. RV cardiac fibroblasts (CFs) were isolated from adult mouse hearts, as described previously [34].

Proliferation and apoptosis assessment

Human PASMCs and PAECs were exposed to Juglone (5-hydroxy-1,4-naphthalenedione) (sc-202675, Santa Cruz Biotechnology, CA, USA) at concentrations between 1 and 10 μM. Proliferation of hPASMCs from non-PAH individuals and patients with IPAH, and hPAECs from healthy control individuals was assayed by monitoring the incorporation of 5-bromo-2deoxyuridine (BrdU) into newly synthesized DNA (Cell Proliferation ELISA BrdU colorimetric kit, Roche, Basel, Switzerland). Apoptosis was assayed using *In Situ* Cell Death Detection Kit, TMR red (Roche, Basel, Switzerland).

Echocardiography and Hemodynamic Measurements

Invasive methods to measure right ventricular systolic pressure (RVSP) and systemic arterial pressure was performed in a blinded manner to all the animals. Transthoracic echocardiographic examination was performed to assess the cardiac function as described previously [35].

Tissue Preparation, Histology, Immunohistostaining

For histology, lungs were fixed with 10% neutral buffered formalin was used. The right lung was snap-frozen. The RV was separated from the left ventricle plus septum (LV+S), and the RV/(LV+S) ratio was calculated as an index of RV hypertrophy.

Statistical Analysis

All data are expressed as mean ± SEM. For comparison of two groups, parametric t-test; for comparisons involving more than two groups one-way ANOVA with post-hoc Newman-Keuls multiple comparisons test were applied. Values of $P < 0.05$ were considered statistically significant.

The details on biospecimen collections and primary cell isolations, siRNA transfections, Luciferase Reporter Assays, Transcription Factor Array, RT-qPCRs, Western Blot analyses, immunostaining and lung morphometry are provided in the Online Data Supplemental.

Results

Peptidyl-prolyl isomerase 1 activation in experimental and human PAH

The expression of peptidyl-prolyl isomerase (Pin1) was examined in lung specimens of patients with idiopathic pulmonary hypertension (IPAH) and non-PAH donor individuals. The immune reactivity of Pin1 was evidently augmented in pulmonary vascular compartments of IPAH patients, in comparison to non-PAH controls (Figure 1a). Co-immunostaining with α-smooth muscle actin (α-SMA) established Pin1 localization in the medial layer of the pulmonary arterial walls of IPAH lungs. Western Blot analyses demonstrated remarkably higher Pin1 expression in IPAH hPASMCs, but not in IPAH hPAECs, as compared to their respective non-PAH control cells (Figure 1b-e). Pin1 expression in IPAH hPASMCs exhibits a significant correlation with mean pulmonary arterial pressure (mPAP). A weak insignificant correlation with pulmonary capillary wedge pressure (PCWP), cardiac index (CI) and systolic pulmonary artery pressure (sPAP) of the IPAH patients was detected (Figure 1f-i). Intriguingly, qPCR analyses of mRNA from the laser-assisted micro-dissected vessels (LMVs) and human lungs exhibited no significant difference of *PIN1* between IPAH and non-PAH controls (Supplemental Figure 1a, b, c).

An accumulation of Pin1 protein in lung homogenates of Sugen5416/hypoxia (SuHx) rats and slight, though no significant enhancement of Pin1 in lungs of mice exposed to chronic hypoxia (HOX), as compared to their respective controls was noted (Figure 1j-m). Hypoxia significantly elevated Pin1 protein accumulation in cultured mouse PASMCs (Supplemental Figure 1d). No significant alterations of *Pin1* mRNA expression have been detected in lungs of SuHx and HOX experimental models of PH (Supplemental Figure 1e, f). Pin1 expression is markedly elevated in pulmonary vessels of both experimental PH models (Supplemental Figure 2a, b).

Pin1 blockage results in suppression of vascular cell proliferation and initiation of cell apoptosis *in vitro*

The effect of pharmacological inhibition of Pin1 by the small molecule inhibitor Juglone, was first investigated on proliferation of hPASMCs. Juglone inhibited platelet-derived growth factor (PDGF-BB)-driven proliferation of both non-PAH hPASMCs and hPASMCs from IPAH patients (Figure 2a). To further support the notion that Pin1 is critically important for PASMC proliferation, siRNA approach targeting Pin1 was employed *in vitro*. The expression of Pin1 was strongly declined in Pin1-silenced hPASMCs, as compared to control transfected cells (Figure 2b,c). The ablation of Pin1 via siRNA or Juglone decreased the expression of Proliferating Cell Nuclear Antigen (PCNA) and Ki-67 in hPASMCs under basal conditions (Figure 2b-d,f, and Supplemental Figure 3a-c). Moreover, Pin1 blockage suppressed the proliferative response of hPASMCs under basal and stimulated (PDGF-BB) conditions (Figure 2e), pointing to its role in cell cycle regulation. Interestingly, the proliferation of hPAECs challenged with fetal bovine serum (FBS) was also markedly inhibited by Juglone and by Pin1-siRNA approach both in control and diseased hPAECs (Figure 2g,h). Blockage of Pin1 by Juglone caused the augmentation of terminal deoxynucleotidyl transferase dUTP nick end labeling (TUNEL)-positive control and diseased hPASMCs (Figure 3a,i and Supplemental Figure 3d,e). Juglone also inhibited the resistance to apoptosis of both control and diseased hPASMCs, as indicated by upregulated expression of pro-apoptotic active cleaved forms of Caspase 3 and Poly (ADP-ribose) polymerase (PARP-1) (Figure 3b-d and j-l). Pin1 inhibition led to the resistance to apoptosis of hPAECs, as determined by elevated number of TUNEL-positive control and diseased hPAECs (Figure 3e,o and Supplemental Figure 3f,g), increased expression of active Caspase 3 and PARP-1 apoptotic markers (Figure 3f-h and p-r and Supplemental Figure 2g, h). The decrease in PCNA have been detected in Juglone-treated IPAH hPASMCs (Figure 3m,n), while no obvious change in IPAH hPAECs was observed (Figure 3s,t). Taken together our data suggest that Pin1 inhibition may possess positive therapeutic impacts in PAH.

Pin1 controls the activity of a multitude of transcription factors

Next, we determined the effect of various PH-inducing growth factors/pro-inflammatory cytokines on Pin1 expression in hPASMCs. Induction of Pin1 in hPASMCs was observed exclusively after stimulation with PDGF-BB, Epidermal growth factor (EGF), and the Growth Medium (GM), a mixture of growth factors,

compared to untreated control cells (Figure 4a). Interestingly, neither members of Bone Morphogenetic Protein family (BMPs) nor pro-inflammatory cytokines (Tumor Necrosis Factor-α, Interleukin 6) recognizably modified Pin1 expression, indicative of a selective mode of Pin1 regulation in hPASMCs (Supplemental Figure 4a-d). As Pin1 driven isomerization has been reported to play a significant role in the activity of various transcription factors (TFs) facilitating multiple proliferation-supporting pathways [8, 36], we monitored the activity of a set of 96 TFs from Pin1-silenced and Juglone-treated hPASMCs. The depletion of Pin1 reduced the activity of growth-promoting and increased the activity of proliferation-restraining TFs (Figure 4b). Several transcription factors and transcriptional co-activators implicated in PH and RV dysfunction such as Hypoxia-inducible factor (HIF), Nuclear factor kappa B (NF-κB), SMAD family (SMADs), Signal transducers and activators of transcription (STATs) were dysregulated upon Pin1 inactivation either by knock-down of Pin1 or Juglone exposure (Figure 4b,c). A remarkable decrease of HIF-1α in control and IPAH hPASMCs and upregulation of tumor suppressor C/EBPα in control hPASMCs was detected in Pin1-silenced hypoxia-treated hPASMCs (Figure 4d-g). Hypoxia increased the hypoxia responsive element (HRE)-luciferase activity was strongly suppressed in Pin1-silenced hPASMCs (Figure 4f).

Juglone reduces Pulmonary Vascular Remodeling and improves RV Function in Sugen/Hypoxia-induced PAH

The effect of Pin1 inhibition was examined in the SuHx rat model of PAH (Figure 5a), highly resembling some forms of human PAH [37]. Juglone administration (1.5 mg/kg per body weight) from day 21 to 35 significantly reduced right ventricular systolic pressure (RVSP) in comparison to Placebo-treated control rats (Figure 5b). A decrease of RVSP was accompanied by diminished RV hypertrophy, as determined by Fulton index (the ratio of RV weight to the weight of left ventricle plus septum [RV/LV+S]), compared with Placebo-treated control rats (Figure 5c). Administration of Juglone did not affect the systemic blood pressure (Supplemental Figure 4e). The decrease in RVSP and RV hypertrophy in Juglone-treated rats was followed by the diminution in RV dilation (RVID), an increase in Tricuspid Annular Plane Systolic Excursion (TAPSE), the insignificant rise of Cardiac Index (CI), and a severe drop in total Pulmonary Vascular Resistance Index (PVRI) (Figure 5d-g). Next, we

determined the effect of Juglone treatment on pulmonary vascular remodeling. Treatment of rats with Juglone reduced the number of fully muscularized and increased the number of non-muscularized pulmonary arteries in the rat lungs, in comparison to Placebo-treated control rats (Figure 5h and Supplemental 5a). Furthermore, Pin1 inhibition resulted in a strong and significant decrease in medial wall thickness, in a total number of fully occluded vessels, and PCNA-positive cells per vessel (Figure 5i, j, k, and Supplemental 5b-d), indicative of inhibition of proliferation and beneficial impact on pulmonary vessel remodeling. Next, we investigated the impact of Pin1 inhibition on right heart remodeling. Sircol assay staining of RV sections from Juglone-treated rats revealed that Pin1 inhibition provided beneficial, although non-significant effects on RV fibrosis, in comparison to Placebo-treated control rats (Figure 5k and Supplemental 5e). Transforming growth factor beta-1 treatment of cardiac fibroblasts (CFs) resulted in the accumulation of collagens, which was abolished by co-treatment with Juglone (Figure 5l). Thus, the impairment of fibrosis in the RVs was associated with the reduction of collagen synthesis and secretion in CFs, indicating that Pin1 is an endogenous regulator of fibrosis in right heart remodeling, secondary to PH. Juglone administration strongly, though not significantly affected the HIF-1α and C/EBPα expression (Supplemental Figure 5f, g). Western Blot analyses of total lung homogenates demonstrated that Pin1 blockage enhanced Cleaved Caspase 3 accumulation and resulted in a clear but insignificant reduction of STAT3 activation (Figure 5n, o). In summary, our data exhibit that Pin1 inhibition improved hemodynamics, RV function, pulmonary vascular and cardiac remodeling in SuHx model of PAH.

Juglone impairs the progression of pulmonary hypertension induced by chronic hypoxia

Next, the impact of Pin1 inhibition in chronic-hypoxia-induced PH was examined (Figure 6a). Mice exposed to 35 days of chronic hypoxia developed PH, indicated by an increase in RVSP and RV hypertrophy (Figure 6b, c). Treatment with Juglone (3 mg/kg per day) from day 21 to 35 resulted in a slight, though not significant reduction of both RVSP and Fulton index, compared to Placebo-treated control mice (Figure 6b, c). No changes in systemic blood pressure have been noted after Juglone administration (Supplemental Figure 6e). A slight increase in TAPSE (Figure 6e), has been correlated with a substantial increase of CI (Figure 6f) and marked

reduction in PVRI in Juglone-treated mice, as compared to Placebo-treated control animals (Figure 6g). Juglone-treated mice demonstrated improved vessel remodeling, evidenced by the significant reduction of fully muscularized pulmonary arteries and medial wall thickness (Figure 6h, i and Supplemental Figure 6a, b). Next, we sought to determine the impact of Juglone on apoptosis occurrence in mouse lungs *in vivo* and *ex vivo.* Apoptosis was markedly and significantly increased in the lungs of Juglone-treated mice, as determined by Fluorescence Molecular Tomography (FMT) *in vivo* analyses employing Annexin-Vivo™ 750 probe (marks the early stages of apoptosis) (Figure 6j, k). The *ex vivo* analyses also revealed a significant increase in TUNEL-positive vascular cells of Juglone-treated mice (Figure 6l and Supplemental Figure 6c) and a decrease in Ki-67+ vascular cells (Figure 6j and Supplemental Figure 6d). Juglone did not affect the Pin1 protein expression in Juglone-treated mice (Supplemental Figure 6e). Taken together our data demonstrate that Pin1 inhibition improves RV function and reverses pulmonary vascular remodeling in hypoxia-exposed mice.

Discussion

The emergence and development of PAH encompass complex pathological mechanisms, whereas successful therapeutical treatment of the disease currently remains a major challenge. Here we show a marked elevation in the expression of peptidyl-prolyl cis*/*trans isomerase (Pin1) in lungs of experimental PH and hPASMCs of patients with PAH. Pin1 abundance in PASMCs strongly correlates with the mean pulmonary artery pressure of IPAH patients. Inhibition of Pin1 by a naphthoquinone Juglone efficiently ameliorated both hypoxia and non-hypoxia-induced PAH, evidenced by improved hemodynamics, RV function, and pulmonary vascular remodeling, verifying that inhibition of disease progression associated with Juglone-mediated effects on Pin1. These data are in correlation with *in vitro* results, in which Pin1 blockage diminished proliferation and declined the resistance to apoptosis of hPASMCs and hPAECs. Pin1 is an enzyme, which catalyzes the *cis*/*trans* conversion of its substrate upon binding to the pSer/Thr-Pro consensus motifs within the target [10, 38, 39]. Pin1-driven isomerization of multiple substrates results in various biological outcomes [22, 40], providing an alternate path of control of abundant signaling cascades under different cellular conditions [14, 41]. Pin1

controls the activity of a range of transcription factors (TFs) and could provide a pivotal switch in disease pathogenesis by regulating the gene expression of its transcriptional substrates [42]. Pin1 contributes to cell cycle control of various diseases [22, 40, 43, 44], partially by regulating the nucleo-cytoplasmic shuttling and activity of TFs, which control cell proliferation and inflammatory response. For example, Pin1 mediated nuclear shuttling and isomerization of β-catenin leads to upregulation of its target genes, Cyclin D1 and c-Myc [45]. Pin1 promoted nuclear accumulation of NF-κB subunit RelA, via inhibition its binding to IκBα, enhances cell growth and inflammatory cytokine production [46]. Pin1 could also sequester the cytoplasmic shuttling of a tumor suppressor of forkhead family of transcription factor 4 (FOXO4), resulting in a decrease of its transcriptional activity toward its target genes, as p27kip1 [47]. Pin1 can regulate the stability of plethora of TFs, key regulators of PAH emergence and progression, as FOXOM [48, 49]; Peroxisome Proliferator-Activated Receptor γ [50, 51], HIF [52, 53], Estrogen Receptor α [54, 55] and transcriptional co-activatiors, as Notch [56, 57]. Moreover, Pin1 reported increasing the stability and transcriptional activity of bromodomain-containing protein 4 (BRD4), one of the critical epigenetic drivers for PAH [58, 59]. In our study TF profiling arrays revealed that Pin1 efficiently controls the activity of key TFs, implicated in PH emergence and development, suggesting that Pin1 is an important endogenous integrator in the context of PAH. Specifically, we show that siRNA-mediated or Juglone-treated depletion of Pin1 resulted in a strong decrease in transcriptional activity of crucial TFs, which have been previously implicated in cell proliferation and migration, chronic inflammation, and tissue remodeling (STAT3, HIF, NF-κB, and SMADs) [60-62]. This goes in agreement with the observations that, Pin1 blockage resulted in a marked decrease in proliferative responses of hPASMCs and hPAECs, indicating that endogenous Pin1 contributes to the pseudo-malignant phenotype of the disease. Anti-apoptotic resistance of vascular cells is another hallmark of PAH [3] and Pin1 has been already implicated in cell death in various pathological conditions [63, 64]. Importantly, a strong and significant initiation of apoptosis and successive inhibition of vascular cell proliferation distinguished upon Pin1 deletion was tightly correlated with a substantial initiation of cell death in lungs of chronic-hypoxia-induced PH. Knock-down of Pin1 in pulmonary vascular cells, resulted in inhibition of proliferative and activation of pro-apoptotic responses, implicating the endogenous Pin1 for PH development. Myocardial apoptosis has

been associated with RV dysfunction and fibrosis [65], thus apoptosis may provide a detrimental impact on RV function. In our study, apoptosis initiation was exclusively presented in lung vascular cells, and more specifically in SMCs, while FMT did not reveal any apoptotic signal in the heart. Pin1 regulates the intensity and duration of cardiac hypertrophic response [66]. The inhibition of Pin1 alleviated cardiac damage and fibrosis in isoprenaline- and diabetes-induced myocardial fibrosis in rats [67, 68], verifying our data that Pin1 contributes to the development of cardiac remodeling in SuHx-administered rats. Furthermore, recently it was reported that Pin1 blockage reversed the PAH phenotype in PAH microvascular endothelial cells *in vitro* and in PAH rats *in vivo* [69]. Interestingly, our detailed expression analyses of Pin1 indicated inconsistency between mRNA and protein both in experimental, as well as clinical PAH, suggesting that Pin1 protein might be stabilized in the course of the disease. Plk-1, which expression was recently shown to be significantly increased in distal pulmonary arteries and isolated PASMCs from PAH patients (unpublished observations of a group of S. Bonnet) has been reported to stabilize Pin1 protein, which might explain the disparity in mRNA and protein levels of Pin1 in PAH [23].

Juglone along with another naphthoquinone, Plumbagin, is intensively studied in cancer *in vivo* [70-73]. Plumbagin inhibited PAH-hPASMC proliferation and resistance to apoptosis were associated with a decrease in pulmonary artery remodeling, mean pulmonary artery pressure, and RV hypertrophy in experimental PAH rat models via STAT3/NFAT axis [74]. The deletion of Pin1 in hPASMCs in our experiments also resulted in a strong and remarkable decline of both STAT3 and STAT5 activity, suggesting a common for both naphthoquinones routes of regulation.

One of the primary limitations of this study is that the control and PAH-hPAECs were obtained from different sources. The slight variations in the isolations and culturing procedures of these primary cells, therefore, may impact the functional activity of these cells in response to Juglone. Many of naphthoquinones, including Juglone are characterized by pro-oxidant properties. In this regard, Juglone acts not only as a redox-cycling agent, but also as producer of reactive oxygen species [75]. In addition to its pro-oxidant properties, Juglone also possess both the cytotoxic and the genotoxic properties [76], thus the damaging impact of Juglone on health cells cannot be completely ruled out. Pin1 serves as a linkage, between various signaling mechanisms at multiple levels. A proposed Pin1 mechanism in PH has been illustrated in Figure 7.

Our data underscore the importance of Pin1 for controlling the activity of presently uninvestigated for the PAH TFs. A deeper understanding of molecular mechanisms driving Pin1 regulation and the molecular/cellular circuits driven by Pin1 in diseased vascular cells is essential for developing tailored therapeutic concepts focusing on Pin1 inhibition.

Acknowledgments

The authors would like to thank Carina Lepper, Christina Vroom, Ewa Bieniek and Sophia Hattensohl for their technical assistance.

Sources of funding

The authors received funding from the German Research Foundation (DFG) by the CRC1213 (Collaborative Research Center 1213) projects A08, B04 and CP02.

Disclosures

None

Figure legends

Fig.1.

Peptidyl-prolyl isomerase 1 activation in experimental and human PAH. a) Representative immunofluorescence micrograph of human lung sections from control and IPAH patients. Staining was undertaken for Pin1 (green) and vessel identity was visualized by α-smooth muscle actin (αSMA) (red). Scale bar: 50 μm. **b), d)** Protein expression of Pin1 in smooth muscle cells (control=4, IPAH=9) and endothelial cells (control=4, IPAH=5) isolated from pulmonary arteries of control and IPAH patients. Regulation at protein level was analyzed by Western Blot analysis followed by **c), e)** densitometric analysis. **f-i)** Correlation of Pin1 with clinical characteristics of IPAH patients such as, mean pulmonary arterial pressure (mPAP) (n=4; r=0.8177; p=0.0468), pulmonary capillary wedge pressure (PCWP) (n=6; r=-8825; p=0.1175), cardiac index (CI) (n=4; r=-0.8276; p=01724) and systolic pulmonary artery pressure (sPAP) (n=7; r=-0.6285; p=0.1306), respectively. **j), l)** Western Blot analysis of Pin1 in lung homogenates exposed to SuHx (NOX=4, SuHx=4) and chronic-hypoxia respectively (NOX=6, HOX=7) followed by **k), m)** densitometric analysis. Pan-actin is taken as loading control. *p<0.05; ***p<0.001 with Student´s t-test.

Fig.2.

Pin1 blockage results in the suppression of vascular cell proliferation *in vitro*. a) hPASMCs from controls and IPAH patients cultured in SmGM-2 were serum starved and treated with Juglone or DMSO (vehicle) in the presence of PDGF-BB for 24 h. **b)** Representative Western Blots of Pin1 and PCNA expression in control and IPAH hPASMCs followed by **c)** densitometric analysis 24 h after Pin1 mRNA knockdown. Immunofluorescence staining for Ki-67+ cells in **d)** Pin1-silenced and **f)** Juglone-exposed hPASMCs. **g)** hPAECs were serum starved (0.2% FBS in M200) and stimulated with 10% FBS with or without Juglone for 24 h. Proliferation of Pin1-silenced **e)** hPASMCs and **h)** hPAECs of donor control and IPAH patients in presence or absence of **e)** PDGF-BB and **h)** 10% FBS determined by BrdU incorporation. The rate of DNA synthesis for **a)**, **e)**, **g)** and **h)** was examined by

measuring of BrdU incorporation [A_{370nm}]. Statistical analysis was performed using one-way ANOVA with Newman-Keuls post-hoc test for multiple comparisons; **p<0.01, ***p<0.001, ****p<0.0001 *versus* PDGF-BB or 10%FBS treated cells; $^{\#}$p<0.05, $^{\#\#}$p<0.01, $^{\#\#\#}$p<0.001, $^{\#\#\#\#}$p<0.0001 *versus* si scrambled or DMSO-treated cells; §p<0.05, §§ p<0.01, §§§p<0.001 and §§§§p<0.0001 *versus* si scrambled treated or IPAH cells Data from three independent experiments are presented as mean ± SEM.

Fig.3.

Pin1 blockage results in initiation of cell apoptosis *in vitro*. Terminal deoxynucleotidyl transferase dUTP nick end labeling (TUNEL) assay after 24 h treatment with increasing concentration of Juglone of **a)** control and **i)** IPAH hPASMCs, and of **e)** control and **o)** IPAH hPAECs. **b), j), m)** Representative Western Blots and **c)**, **d)**, **k)**, **l), n)** subsequent densitometric analysis of control and IPAH hPASMCs after Juglone treatment. **f), p), s)** Representative Western Blots and **g)**, **h)**, **q)**, **r)**, **t)** subsequent densitometric analysis of control and IPAH hPAECs are presented. *p<0.05; **p<0.01; ***p<0.001 *versus* DMSO-treated control cells. Statistical analysis was performed using one-way ANOVA with Newman-Keuls post-hoc test for multiple comparisons. Data from three independent experiments are presented as mean ± SEM.

Fig.4.

Pin1 controls the activity of multitude of transcription factors. a) Control and IPAH hPASMCs after 24h of serum starvation were subjected to PDGF-BB (50 ng/ml), EGF (5 ng/ml) and Growth Medium (GM) with 5% FBS. Intracellular Pin1 levels were monitored by ELISA. *p<0.05, ****p<0.0001 *versus* control PASMCs; $^{\#\#}$p<0.01, $^{\#\#\#\#}$p<0.0001 *versus* IPAH hPASMCs; §§p<0.01 IPAH hPASMCs versus control hPASMCs. Statistical analysis was performed using one-way ANOVA with Newman-Keuls post-hoc test for multiple comparisons. Data from three independent experiments are presented as mean ± SEM. **b)** Pin1-silenced and Juglone-treated hPASMCs were stimulated with Growth Medium for 24 h and nuclear protein extracts were used for TF activation profile array, presented as log-transformed signals in a volcano plot. **c)** Log-transformed scatter plot of combined TF activation/inactivation

in Pin1-silenced and Juglone-treated hPASMCs. Data from two independent experiments are presented. **d)**, **f)** Western blots and **e)**, **g)** subsequent densitometry analyses of HIF-1α and C/EBPα TFs in Pin1-silenced control and IPAH hPASMCs subjected to hypoxia for 24 h. **i)** Hypoxia-responsive element (HRE) luciferase activity in Pin1-silenced hPASMCs after 24 h of hypoxia. *p<0.05; ****p<0.0001 for NOX si Scr *versus* HOX si Scr; §p<0.05; §§§§p<0.0001 for HOX si Scr *versus* HOX si Pin1. Data from three independent experiments are presented as mean ± SEM.

Fig.5.

Juglone reduces Pulmonary Vascular Remodeling and improves RV Function in Sugen/Hypoxia induced PAH. a) Schematics of the animal treatment. Echocardiography followed by physiological measurements was carried out on Juglone-treated [1.5 mg/kg per BW], placebo-treated Sugen/Hypoxia (SuHx) rats and healthy rats 35 days after initiation of SuHx treatment. **b)** Right ventricular systolic pressure [RVPsys], as measured by right heart catheterization, **c)** ratio of RV mass to mass of left ventricle plus septum [RV/(LV+S)], **d)** right ventricle internal diameter [RVID], **e)** tricuspid annular plane systolic excursion [TAPSE]. (NOX=5, SuHx=5, SuHx+Juglone=9), **f)** cardiac index [CI], and **g)** pulmonary vascular resistance index [PVRI] of the rats as measured by echocardiography. NOX=5, SuHx=4, SuHx+Juglone=9. Ex-vivo analyses of lung tissues for reversal of remodeling and *in vivo* drug efficacy on fibrosis. **h)** The degree of muscularization of small pulmonary arteries (diameter 20-50 µm) was determined by immunohistological stainings for vWF and α-SMA antibodies of lung sections. M: fully muscularized; P: partially muscularized; N: non-muscularized. **i)** and **j)** Lung sections stained with Elastica-van-Gieson to determine medial wall thickness of vessels [%] and occlusion score [%] with a diameter of 20-50 µm. O: open; P: partial; C: closed. NOX=5, SuHx=5, SuHx+Juglone=9. **k)** Quantitative analysis of proliferating cell nuclear antigen (PCNA)- positive cells per vessel in lungs (NOX=4, SuHx=4, SuHx+Juglone=4). **l), m)** Effect of Juglone on RV fibrosis (NOX=5, SuHx=5, SuHx+Juglone=7) and secreted collagen content in isolated cardiac fibroblasts (data from three independent experiments are presented as mean ± SEM). **n)** Western Blot analyses followed by **o)** densitometry of lung homogenates of representative samples from all three experimental groups. NOX=4, SuHx=4, SuHx+Juglone=4.

**p<0.01; ***p<0.001, ****p<0.0001 for SuHx *versus* NOX; §p<0.05; §§p<0.01; §§§p<0.001, §§§§p<0.0001 for SuHx+Juglone *versus* SuHx. Statistical analysis was performed using one-way ANOVA with Newman-Keuls post-hoc test for multiple comparisons.

Fig.6.

Juglone impairs the progression of PH induced by chronic hypoxia in mice. Effect of Juglone on hemodynamics and right heart function in chronic hypoxia mice. **a)** Schematics of the animal treatment. Echocardiography followed by physiological measurements was carried out on Juglone-treated [3 mg/kg per BW], placebo-treated HOX mice and healthy mice 35 days after initiation of hypoxia treatment. **b)** Right ventricular systolic pressure [RVPsys] as measured by right heart catheterization, **c)** ratio of RV mass to mass of left ventricle plus septum [RV/(LV+S)], and **d)** right ventricle internal diameter [RVID] **e)** tricuspid annular plane systolic excursion [TAPSE]. NOX=5, HOX=5, HOX+Juglone=10. **f)** Cardiac index [CI] and **g)** Pulmonary vascular resistance index [PVRI] of the mice as measured by echocardiography. NOX=5, HOX=5, HOX+Juglone=9. Ex-vivo analyses of lung tissues for reversal of remodeling. **h)** and **i)** The degree of muscularization of small pulmonary arteries (diameter 20-70 µm) was determined by immunohistological for vWF and α-SMA of lung sections. M: fully muscularized; P: partially muscularized; N: non-muscularized and lung sections stained with Elastica-van-Gieson was used to determine the medial wall thickness of vessels [%]. **j)** and **k)** Fluorescence in vivo imaging of mice detected by Fluorescence Molecular Tomography (FMT) using Annexin-Vivo 750 and representative images for all three groups. NOX=5, HOX=5, HOX+Juglone=10. Apoptotic and proliferative indices determined by **l)** TUNEL+ (NOX=4, HOX=4, HOX+Juglone=5) and **m)** Ki-67+ cells per vessel in lungs (NOX=5, HOX=5, HOX+Juglone=5). **p<0.01, ***p<0.001, ****p<0.0001 for HOX *versus* NOX; §p<0.05, §§p<0.01, §§§p<0.001, §§§§p<0.001 for HOX+Juglone *versus* HOX. Statistical analysis was performed using one-way ANOVA with Newman-Keuls post-hoc test for multiple comparisons.

Fig.7.

A proposed signaling mechanism of Pin1 in pulmonary hypertension. Aberrant growth factor signaling induces Pin1 leading to isomerization of various target proteins and regulation of transcription factors resulting in proliferation and survival of pulmonary vascular cells. Amplification of pro-proliferative and anti-apoptotic pathways by Pin1 leads to pulmonary vascular remodeling and right ventricular failure and Juglone by inhibiting Pin1 response could provide a potential prevention strategy for pulmonary hypertension. Epidermal growth factor (EGF), Growth factors (GF), Hypoxia-inducible factor 1-alpha (HIF1α), Platelet-derived growth factor-BB (PDGF-BB), Peptidylprolyl cis/trans isomerase, NIMA interacting 1 (Pin1), (Proliferating cell nuclear antigen (PCNA), Right ventricle (RV), Signal transducers and activators of transcription 3 (STAT3).

References

1. Schermuly, R.T., et al., *Mechanisms of disease: pulmonary arterial hypertension.* Nat Rev Cardiol, 2011. **8**(8): p. 443-55.
2. Thenappan, T., et al., *Pulmonary arterial hypertension: pathogenesis and clinical management.* BMJ, 2018. **360**: p. j5492.
3. Guignabert, C., et al., *Pathogenesis of pulmonary arterial hypertension: lessons from cancer.* Eur Respir Rev, 2013. **22**(130): p. 543-51.
4. Vonk Noordegraaf, A., J.A. Groeneveldt, and H.J. Bogaard, *Pulmonary hypertension.* Eur Respir Rev, 2016. **25**(139): p. 4-11.
5. Machado, R.D., et al., *Investigation of second genetic hits at the BMPR2 locus as a modulator of disease progression in familial pulmonary arterial hypertension.* Circulation, 2005. **111**(5): p. 607-13.

6. McLaughlin, V.V. and M.D. McGoon, *Pulmonary arterial hypertension.* Circulation, 2006. **114**(13): p. 1417-31.

7. Yuan, J.X. and L.J. Rubin, *Pathogenesis of pulmonary arterial hypertension: the need for multiple hits.* Circulation, 2005. **111**(5): p. 534-8.

8. Zhou, X.Z. and K.P. Lu, *The isomerase PIN1 controls numerous cancer-driving pathways and is a unique drug target.* Nat Rev Cancer, 2016. **16**(7): p. 463-78.

9. Lu, K.P. and X.Z. Zhou, *The prolyl isomerase PIN1: a pivotal new twist in phosphorylation signalling and disease.* Nat Rev Mol Cell Biol, 2007. **8**(11): p. 904-16.

10. Lu, P.J., et al., *Function of WW domains as phosphoserine- or phosphothreonine-binding modules.* Science, 1999. **283**(5406): p. 1325-8.

11. Feng, D., et al., *Inhibition of p66Shc-mediated mitochondrial apoptosis via targeting prolyl-isomerase Pin1 attenuates intestinal ischemia/reperfusion injury in rats.* Clin Sci (Lond), 2017. **131**(8): p. 759-773.

12. Paneni, F., et al., *Targeting prolyl-isomerase Pin1 prevents mitochondrial oxidative stress and vascular dysfunction: insights in patients with diabetes.* Eur Heart J, 2015. **36**(13): p. 817-28.

13. Zhou, X.Z., et al., *Pin1-dependent prolyl isomerization regulates dephosphorylation of Cdc25C and tau proteins.* Mol Cell, 2000. **6**(4): p. 873-83.

14. Liou, Y.C., X.Z. Zhou, and K.P. Lu, *Prolyl isomerase Pin1 as a molecular switch to determine the fate of phosphoproteins.* Trends Biochem Sci, 2011. **36**(10): p. 501-14.

15. Chen, Y., et al., *Prolyl isomerase Pin1: a promoter of cancer and a target for therapy.* Cell Death Dis, 2018. **9**(9): p. 883.

16. Perrucci, G.L., et al., *Peptidyl-prolyl isomerases: a full cast of critical actors in cardiovascular diseases.* Cardiovasc Res, 2015. **106**(3): p. 353-64.

17. Zannini, A., et al., *Oncogenic Hijacking of the PIN1 Signaling Network.* Front Oncol, 2019. **9**: p. 94.

18. Crenshaw, D.G., et al., *The mitotic peptidyl-prolyl isomerase, Pin1, interacts with Cdc25 and Plx1.* EMBO J, 1998. **17**(5): p. 1315-27.

19. Li, H., et al., *Pin1 contributes to cervical tumorigenesis by regulating cyclin D1 expression.* Oncol Rep, 2006. **16**(3): p. 491-6.

20. Liou, Y.C., et al., *Loss of Pin1 function in the mouse causes phenotypes resembling cyclin D1-null phenotypes.* Proc Natl Acad Sci U S A, 2002. **99**(3): p. 1335-40.

21. Yeh, E.S., B.O. Lew, and A.R. Means, *The loss of PIN1 deregulates cyclin E and sensitizes mouse embryo fibroblasts to genomic instability.* J Biol Chem, 2006. **281**(1): p. 241-51.

22. Shen, M., et al., *The essential mitotic peptidyl-prolyl isomerase Pin1 binds and regulates mitosis-specific phosphoproteins.* Genes Dev, 1998. **12**(5): p. 706-20.

23. Eckerdt, F., et al., *Polo-like kinase 1-mediated phosphorylation stabilizes Pin1 by inhibiting its ubiquitination in human cells.* J Biol Chem, 2005. **280**(44): p. 36575-83.

24. Rizzolio, F., et al., *Retinoblastoma tumor-suppressor protein phosphorylation and inactivation depend on direct interaction with Pin1.* Cell Death Differ, 2012. **19**(7): p. 1152-61.

25. Pulikkan, J.A., et al., *Elevated PIN1 expression by C/EBPalpha-p30 blocks C/EBPalpha-induced granulocytic differentiation through c-Jun in AML.* Leukemia, 2010. **24**(5): p. 914-23.

26. Blaydes, J.P., et al., *Stoichiometric phosphorylation of human p53 at Ser315 stimulates p53-dependent transcription.* J Biol Chem, 2001. **276**(7): p. 4699-708.

27. Wulf, G.M., et al., *Role of Pin1 in the regulation of p53 stability and p21 transactivation, and cell cycle checkpoints in response to DNA damage.* J Biol Chem, 2002. **277**(50): p. 47976-9.

28. Reineke, E.L., et al., *Degradation of the tumor suppressor PML by Pin1 contributes to the cancer phenotype of breast cancer MDA-MB-231 cells.* Mol Cell Biol, 2008. **28**(3): p. 997-1006.

29. Shen, Z.J., S. Esnault, and J.S. Malter, *The peptidyl-prolyl isomerase Pin1 regulates the stability of granulocyte-macrophage colony-stimulating factor mRNA in activated eosinophils.* Nat Immunol, 2005. **6**(12): p. 1280-7.

30. Hennig, L., et al., *Selective inactivation of parvulin-like peptidyl-prolyl cis/trans isomerases by juglone.* Biochemistry, 1998. **37**(17): p. 5953-60.

31. Weissmann, N., et al., *Classical transient receptor potential channel 6 (TRPC6) is essential for hypoxic pulmonary vasoconstriction and alveolar gas exchange.* Proc Natl Acad Sci U S A, 2006. **103**(50): p. 19093-8.

32. Novoyatleva, T., et al., *Evidence for the Fucoidan/P-Selectin Axis as a Therapeutic Target in Hypoxia-induced Pulmonary Hypertension.* Am J Respir Crit Care Med, 2019. **199**(11): p. 1407-1420.

33. Perros, F., et al., *Nebivolol for improving endothelial dysfunction, pulmonary vascular remodeling, and right heart function in pulmonary hypertension.* J Am Coll Cardiol, 2015. **65**(7): p. 668-80.

34. Novoyatleva, T., et al., *Deletion of Fn14 receptor protects from right heart fibrosis and dysfunction.* Basic Res Cardiol, 2013. **108**(2): p. 325.

35. Kojonazarov, B., et al., *Effects of multikinase inhibitors on pressure overload-induced right ventricular remodeling.* Int J Cardiol, 2013. **167**(6): p. 2630-7.

36. Lu, Z. and T. Hunter, *Prolyl isomerase Pin1 in cancer.* Cell Res, 2014. **24**(9): p. 1033-49.

37. Colvin, K.L. and M.E. Yeager, *Animal Models of Pulmonary Hypertension: Matching Disease Mechanisms to Etiology of the Human Disease.* J Pulm Respir Med, 2014. **4**(4).

38. Rotin, D., *WW (WWP) domains: from structure to function.* Curr Top Microbiol Immunol, 1998. **228**: p. 115-33.

39. Ingham, R.J., et al., *WW domains provide a platform for the assembly of multiprotein networks.* Mol Cell Biol, 2005. **25**(16): p. 7092-106.

40. Lu, K.P., S.D. Hanes, and T. Hunter, *A human peptidyl-prolyl isomerase essential for regulation of mitosis.* Nature, 1996. **380**(6574): p. 544-7.

41. Lu, K.P., Y.C. Liou, and X.Z. Zhou, *Pinning down proline-directed phosphorylation signaling.* Trends Cell Biol, 2002. **12**(4): p. 164-72.

42. Hu, X. and L.F. Chen, *Pinning Down the Transcription: A Role for Peptidyl-Prolyl cis-trans Isomerase Pin1 in Gene Expression.* Front Cell Dev Biol, 2020. **8**: p. 179.

43. Cheng, C.W. and E. Tse, *PIN1 in Cell Cycle Control and Cancer.* Front Pharmacol, 2018. **9**: p. 1367.

44. Yeh, E.S. and A.R. Means, *PIN1, the cell cycle and cancer.* Nat Rev Cancer, 2007. **7**(5): p. 381-8.

45. Ryo, A., et al., *Pin1 regulates turnover and subcellular localization of beta-catenin by inhibiting its interaction with APC.* Nat Cell Biol, 2001. **3**(9): p. 793-801.

46. Ryo, A., et al., *Regulation of NF-kappaB signaling by Pin1-dependent prolyl isomerization and ubiquitin-mediated proteolysis of p65/RelA.* Mol Cell, 2003. **12**(6): p. 1413-26.

47. Brenkman, A.B., et al., *The peptidyl-isomerase Pin1 regulates p27kip1 expression through inhibition of Forkhead box O tumor suppressors.* Cancer Res, 2008. **68**(18): p. 7597-605.

48. Kruiswijk, F., et al., *Targeted inhibition of metastatic melanoma through interference with Pin1-FOXM1 signaling.* Oncogene, 2016. **35**(17): p. 2166-77.

49. Bourgeois, A., et al., *FOXM1 promotes pulmonary artery smooth muscle cell expansion in pulmonary arterial hypertension.* J Mol Med (Berl), 2018. **96**(2): p. 223-235.

50. Fujimoto, Y., et al., *Proline cis/trans-isomerase Pin1 regulates peroxisome proliferator-activated receptor gamma activity through the direct binding to the activation function-1 domain.* J Biol Chem, 2010. **285**(5): p. 3126-32.

51. Zhang, D., et al., *Activation of PPAR-gamma ameliorates pulmonary arterial hypertension via inducing heme oxygenase-1 and p21(WAF1): an in vivo study in rats.* Life Sci, 2014. **98**(1): p. 39-43.

52. Han, H.J., et al., *Peptidyl Prolyl Isomerase PIN1 Directly Binds to and Stabilizes Hypoxia-Inducible Factor-1alpha.* PLoS One, 2016. **11**(1): p. e0147038.

53. Pullamsetti, S.S., et al., *Hypoxia-inducible factor signaling in pulmonary hypertension.* J Clin Invest, 2020. **130**(11): p. 5638-5651.

54. Rajbhandari, P., et al., *Peptidylprolyl Isomerase Pin1 Directly Enhances the DNA Binding Functions of Estrogen Receptor alpha.* J Biol Chem, 2015. **290**(22): p. 13749-62.

55. Frump, A.L., et al., *17beta-Estradiol and estrogen receptor alpha protect right ventricular function in pulmonary hypertension via BMPR2 and apelin.* J Clin Invest, 2021. **131**(6).

56. Rustighi, A., et al., *The prolyl-isomerase Pin1 is a Notch1 target that enhances Notch1 activation in cancer.* Nat Cell Biol, 2009. **11**(2): p. 133-42.

57. Dabral, S., et al., *Notch1 signalling regulates endothelial proliferation and apoptosis in pulmonary arterial hypertension.* Eur Respir J, 2016. **48**(4): p. 1137-1149.

58. Hu, X., et al., *Prolyl isomerase PIN1 regulates the stability, transcriptional activity and oncogenic potential of BRD4.* Oncogene, 2017. **36**(36): p. 5177-5188.

59. Van der Feen, D.E., et al., *Multicenter Preclinical Validation of BET Inhibition for the Treatment of Pulmonary Arterial Hypertension.* Am J Respir Crit Care Med, 2019. **200**(7): p. 910-920.

60. Pullamsetti, S.S., et al., *Transcription factors, transcriptional coregulators, and epigenetic modulation in the control of pulmonary vascular cell phenotype: therapeutic implications for pulmonary hypertension (2015 Grover Conference series).* Pulm Circ, 2016. **6**(4): p. 448-464.

61. Sysol, J.R., V. Natarajan, and R.F. Machado, *PDGF induces SphK1 expression via Egr-1 to promote pulmonary artery smooth muscle cell proliferation.* Am J Physiol Cell Physiol, 2016. **310**(11): p. C983-92.

62. Firth, A.L., et al., *Upregulation of Oct-4 isoforms in pulmonary artery smooth muscle cells from patients with pulmonary arterial hypertension.* Am J Physiol Lung Cell Mol Physiol, 2010. **298**(4): p. L548-57.

63. Becker, E.B. and A. Bonni, *Pin1 in neuronal apoptosis.* Cell Cycle, 2007. **6**(11): p. 1332-5.

64. Ryo, A., et al., *A suppressive role of the prolyl isomerase Pin1 in cellular apoptosis mediated by the death-associated protein Daxx.* J Biol Chem, 2007. **282**(50): p. 36671-81.

65. Zungu-Edmondson, M., et al., *Modulators of right ventricular apoptosis and contractility in a rat model of pulmonary hypertension.* Cardiovasc Res, 2016. **110**(1): p. 30-9.

66. Toko, H., et al., *Regulation of cardiac hypertrophic signaling by prolyl isomerase Pin1.* Circ Res, 2013. **112**(9): p. 1244-52.

67. Wu, X., et al., *Pin1 facilitates isoproterenolinduced cardiac fibrosis and collagen deposition by promoting oxidative stress and activating the MEK1/2ERK1/2 signal transduction pathway in rats.* Int J Mol Med, 2018. **41**(3): p. 1573-1583.

68. Liu, X., et al., *Inhibition of Pin1 alleviates myocardial fibrosis and dysfunction in STZ-induced diabetic mice.* Biochem Biophys Res Commun, 2016. **479**(1): p. 109-15.

69. *Correction to: Extracellular Cyclophilin A, Especially Acetylated, Causes Pulmonary Hypertension by Stimulating Endothelial Apoptosis, Redox Stress, and Inflammation.* Arterioscler Thromb Vasc Biol, 2017. **37**(6): p. e68.

70. Sugie, S., et al., *Inhibitory effects of plumbagin and juglone on azoxymethane-induced intestinal carcinogenesis in rats.* Cancer Lett, 1998. **127**(1-2): p. 177-83.

71. Wang, P., et al., *ROS -mediated p53 activation by juglone enhances apoptosis and autophagy in vivo and in vitro.* Toxicol Appl Pharmacol, 2019. **379**: p. 114647.

72. Wu, J., et al., *Juglone induces apoptosis of tumor stem-like cells through ROS-p38 pathway in glioblastoma.* BMC Neurol, 2017. **17**(1): p. 70.

73. Xu, M., et al., *Overexpression of PIN1 Enhances Cancer Growth and Aggressiveness with Cyclin D1 Induction in EBV-Associated Nasopharyngeal Carcinoma.* PLoS One, 2016. **11**(6): p. e0156833.

74. Courboulin, A., et al., *Plumbagin reverses proliferation and resistance to apoptosis in experimental PAH.* Eur Respir J, 2012. **40**(3): p. 618-29.

75. Kappus, H. and H. Sies, *Toxic drug effects associated with oxygen metabolism: redox cycling and lipid peroxidation.* Experientia, 1981. **37**(12): p. 1233-41.

76. Ahmad, T. and Y.J. Suzuki, *Juglone in Oxidative Stress and Cell Signaling.* Antioxidants (Basel), 2019. **8**(4).

Fig.1

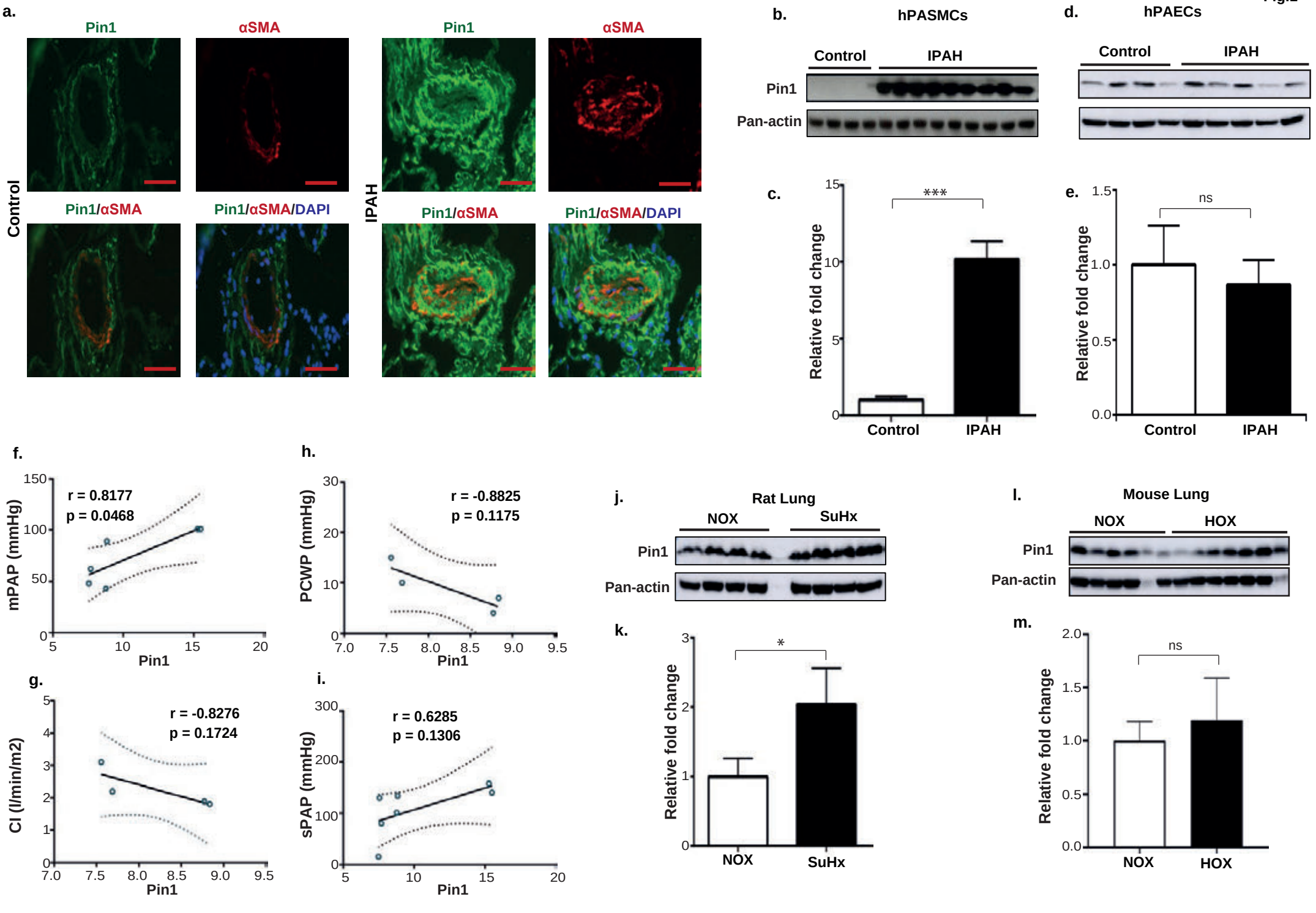
a.
Pin1
αSMA
Pin1
αSMA
Control
IPAH
Pin1/αSMA
Pin1/αSMA/DAPI
Pin1/αSMA
Pin1/αSMA/DAPI
b.
hPASMCs
Control
IPAH
Pin1
Pan-actin
d.
hPAECs
Control
IPAH
c.
***
Relative fold change
Control
IPAH
e.
ns
Relative fold change
Control
IPAH
f.
r = 0.8177
p = 0.0468
mPAP (mmHg)
Pin1
h.
r = -0.8825
p = 0.1175
PCWP (mmHg)
Pin1
g.
r = -0.8276
p = 0.1724
CI (l/min/m2)
Pin1
i.
r = 0.6285
p = 0.1306
sPAP (mmHg)
Pin1
j.
Rat Lung
NOX
SuHx
Pin1
Pan-actin
k.
*
Relative fold change
NOX
SuHx
l.
Mouse Lung
NOX
HOX
Pin1
Pan-actin
m.
ns
Relative fold change
NOX
HOX

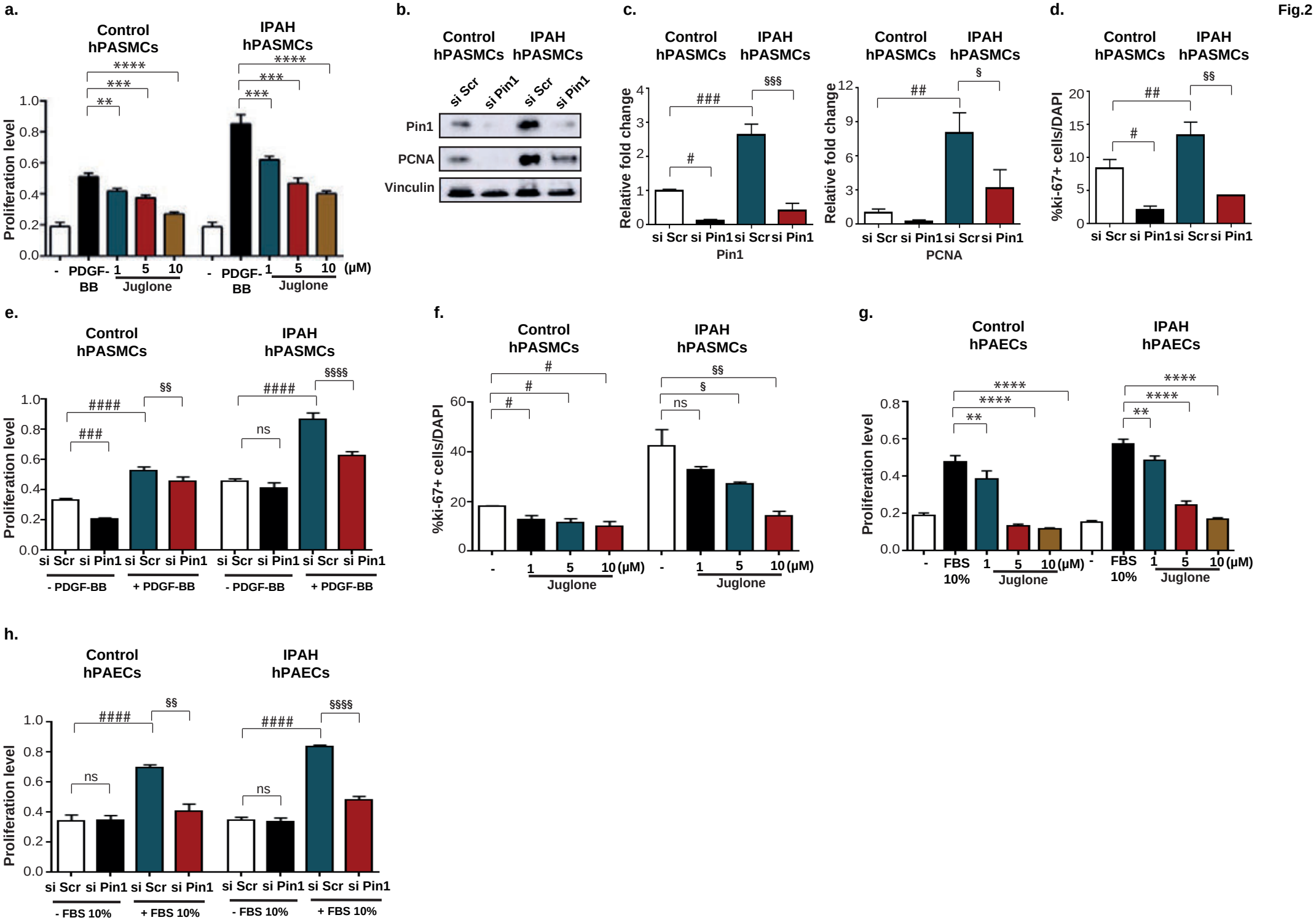
a.
Control hPASMCs
IPAH hPASMCs
Proliferation level
PDGF-BB
Juglone (μM)
b.
Control hPASMCs
IPAH hPASMCs
si Scr
si Pin1
Pin1
PCNA
Vinculin
c.
Control hPASMCs
IPAH hPASMCs
Relative fold change
Pin1
PCNA
d.
%ki-67+ cells/DAPI
e.
Control hPASMCs
IPAH hPASMCs
Proliferation level
- PDGF-BB
+ PDGF-BB
f.
Control hPASMCs
IPAH hPASMCs
%ki-67+ cells/DAPI
Juglone
g.
Control hPAECs
IPAH hPAECs
Proliferation level
FBS 10%
Juglone
h.
Control hPAECs
IPAH hPAECs
Proliferation level
- FBS 10%
+ FBS 10%

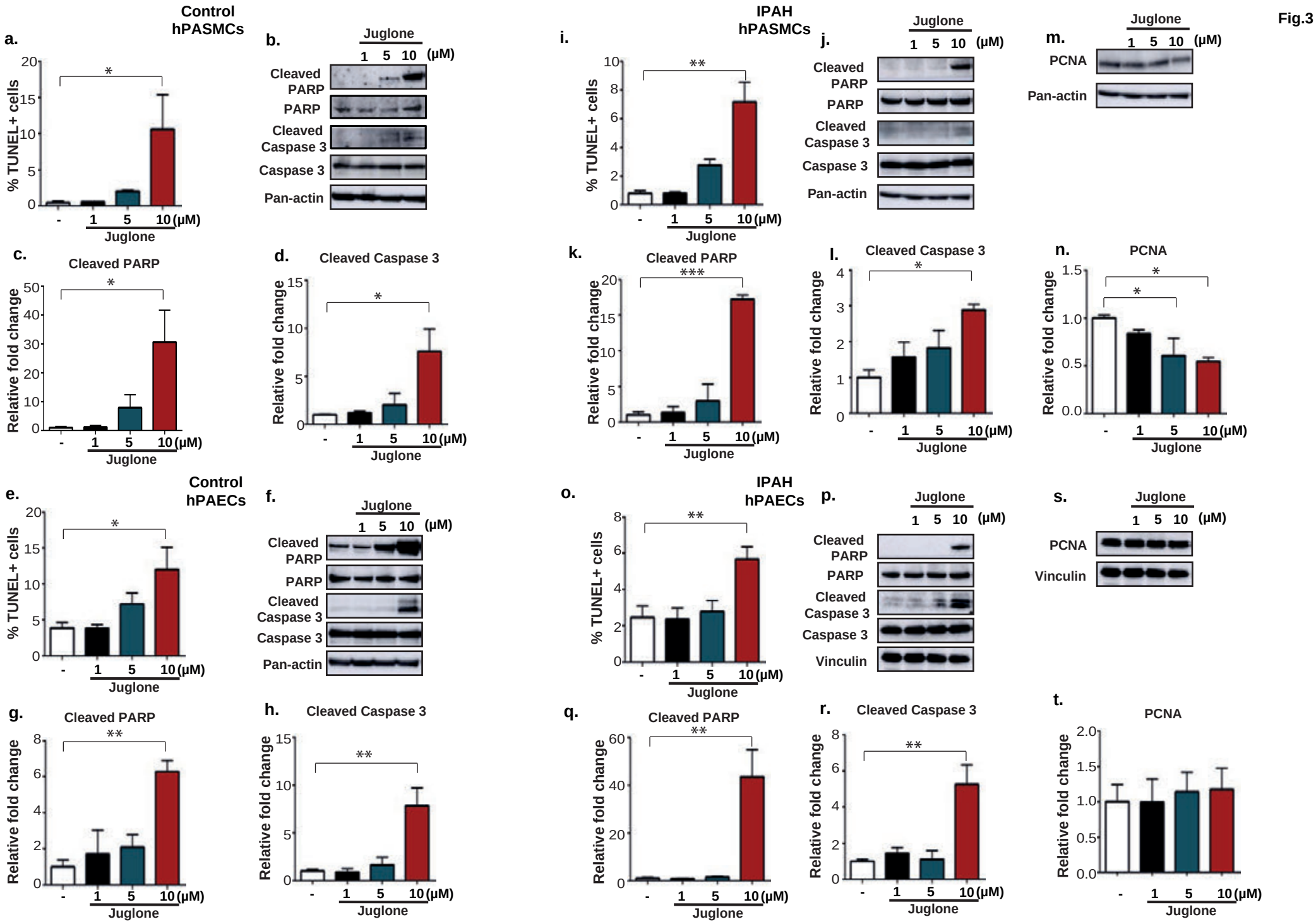
Fig.3
Control hPASMCs
IPAH hPASMCs
Control hPAECs
IPAH hPAECs
a.
b.
c.
d.
e.
f.
g.
h.
i.
j.
k.
l.
m.
n.
o.
p.
q.
r.
s.
t.
% TUNEL+ cells
Relative fold change
Juglone
1 5 10 (μM)
Cleaved PARP
PARP
Cleaved Caspase 3
Caspase 3
Pan-actin
PCNA
Vinculin

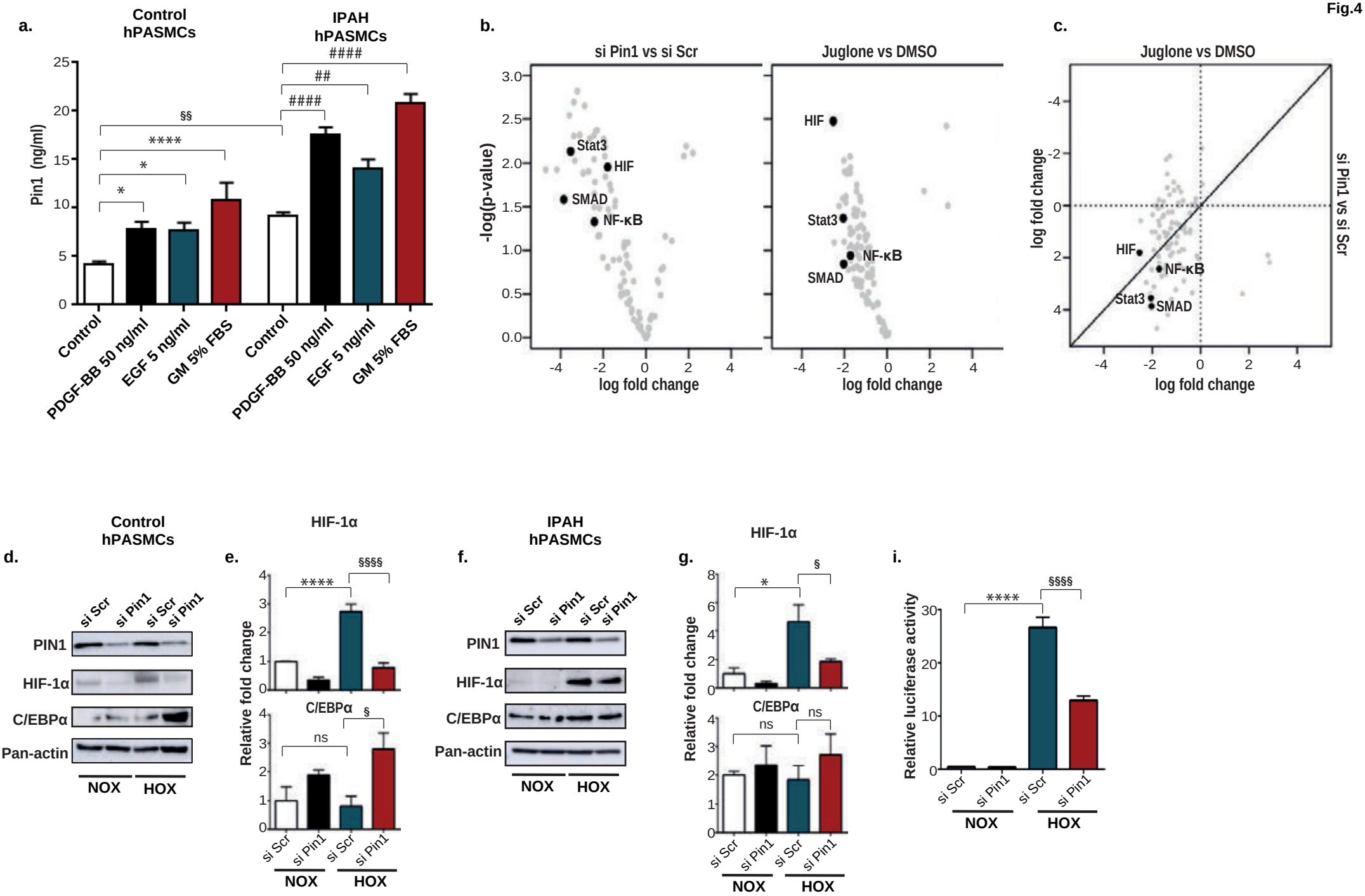
a.
Control hPASMCs
IPAH hPASMCs
Pin1 (ng/ml)
Control
PDGF-BB 50 ng/ml
EGF 5 ng/ml
GM 5% FBS
b.
si Pin1 vs si Scr
Juglone vs DMSO
-log(p-value)
log fold change
HIF
Stat3
SMAD
NF-κB
c.
Juglone vs DMSO
si Pin1 vs si Scr
log fold change
d.
Control hPASMCs
PIN1
HIF-1α
C/EBPα
Pan-actin
si Scr
si Pin1
NOX
HOX
e.
HIF-1α
C/EBPα
Relative fold change
ns
f.
IPAH hPASMCs
g.
HIF-1α
C/EBPα
Relative fold change
i.
Relative luciferase activity

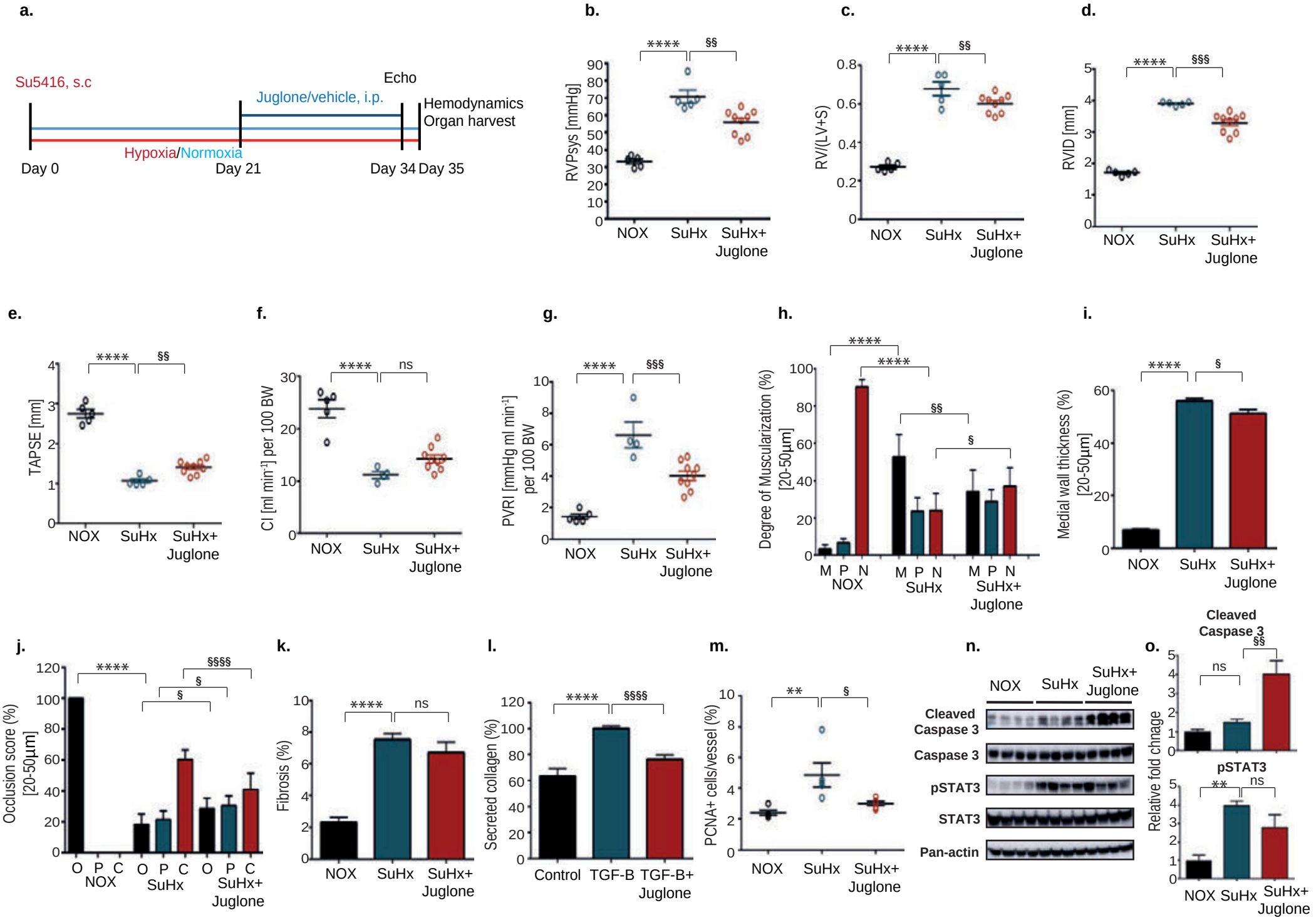
a.
Su5416, s.c
Echo
Juglone/vehicle, i.p.
Hemodynamics
Organ harvest
Hypoxia/Normoxia
Day 0
Day 21
Day 34 Day 35
b.
RVPsys [mmHg]
c.
RV/(LV+S)
d.
RVID [mm]
e.
TAPSE [mm]
f.
CI [ml min-1] per 100 BW
g.
PVRI [mmHg ml min-1] per 100 BW
h.
Degree of Muscularization (%) [20-50µm]
M P N
i.
Medial wall thickness (%) [20-50µm]
NOX
SuHx
SuHx+ Juglone
j.
Occlusion score (%) [20-50µm]
O P C
k.
Fibrosis (%)
l.
Secreted collagen (%)
Control
TGF-B
TGF-B+ Juglone
m.
PCNA+ cells/vessel (%)
n.
Cleaved Caspase 3
Caspase 3
pSTAT3
STAT3
Pan-actin
o.
Relative fold chnage
ns

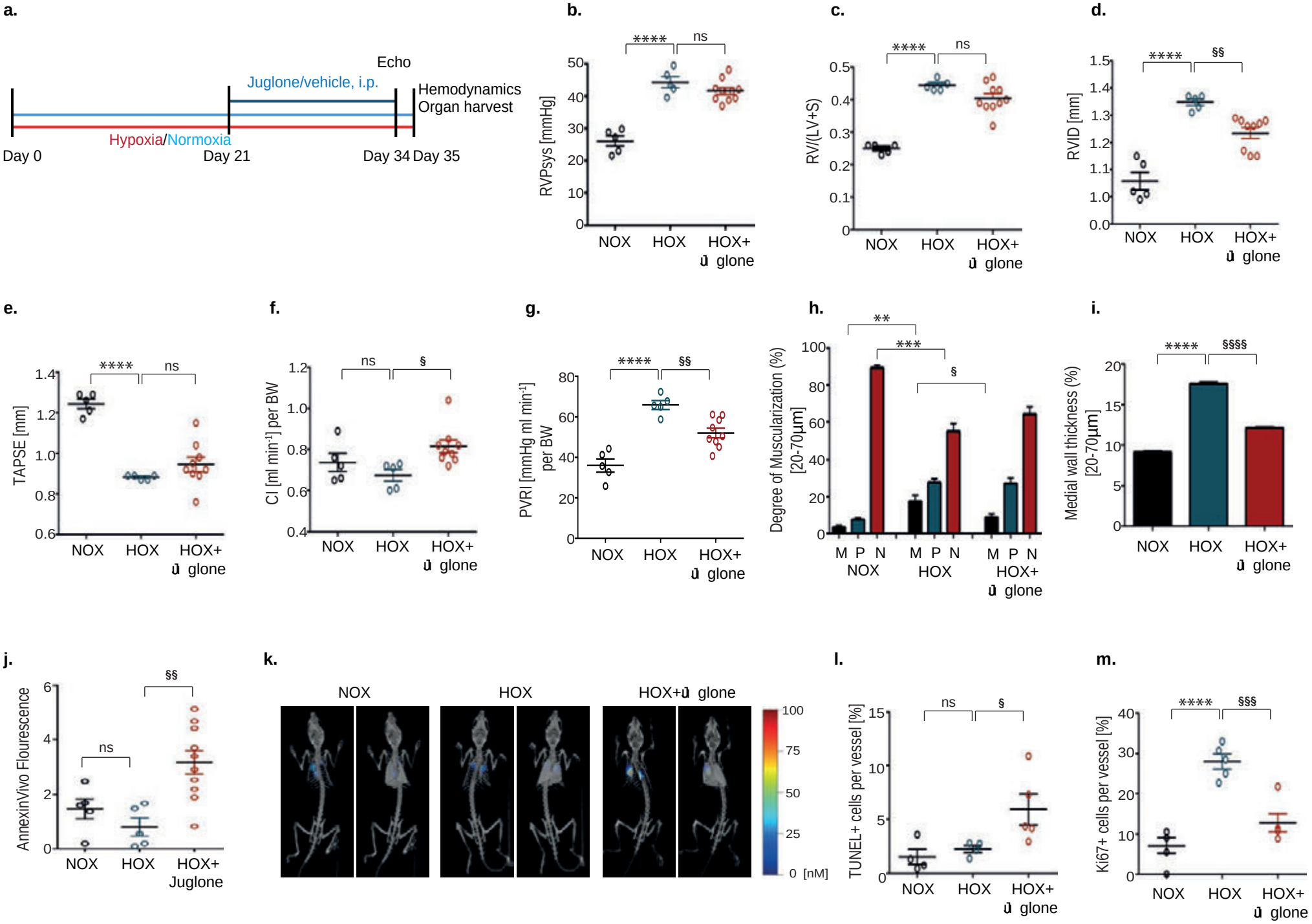
a.
Echo
Juglone/vehicle, i.p.
Hemodynamics
Organ harvest
Hypoxia/Normoxia
Day 0
Day 21
Day 34 Day 35
b.
RVPsys [mmHg]
c.
RV/(LV+S)
d.
RVID [mm]
e.
TAPSE [mm]
f.
CI [ml min-1] per BW
g.
PVRI [mmHg ml min-1] per BW
h.
Degree of Muscularization (%) [20-70µm]
M P N
NOX
HOX
HOX+ glone
i.
Medial wall thickness (%) [20-70µm]
j.
AnnexinVivo Flourescence
Juglone
k.
NOX
HOX
HOX+ glone
100
75
50
25
0 [nM]
l.
TUNEL+ cells per vessel [%]
m.
Ki67+ cells per vessel [%]
ns
§
§§
§§§
§§§§
**
***
****

Fig.7

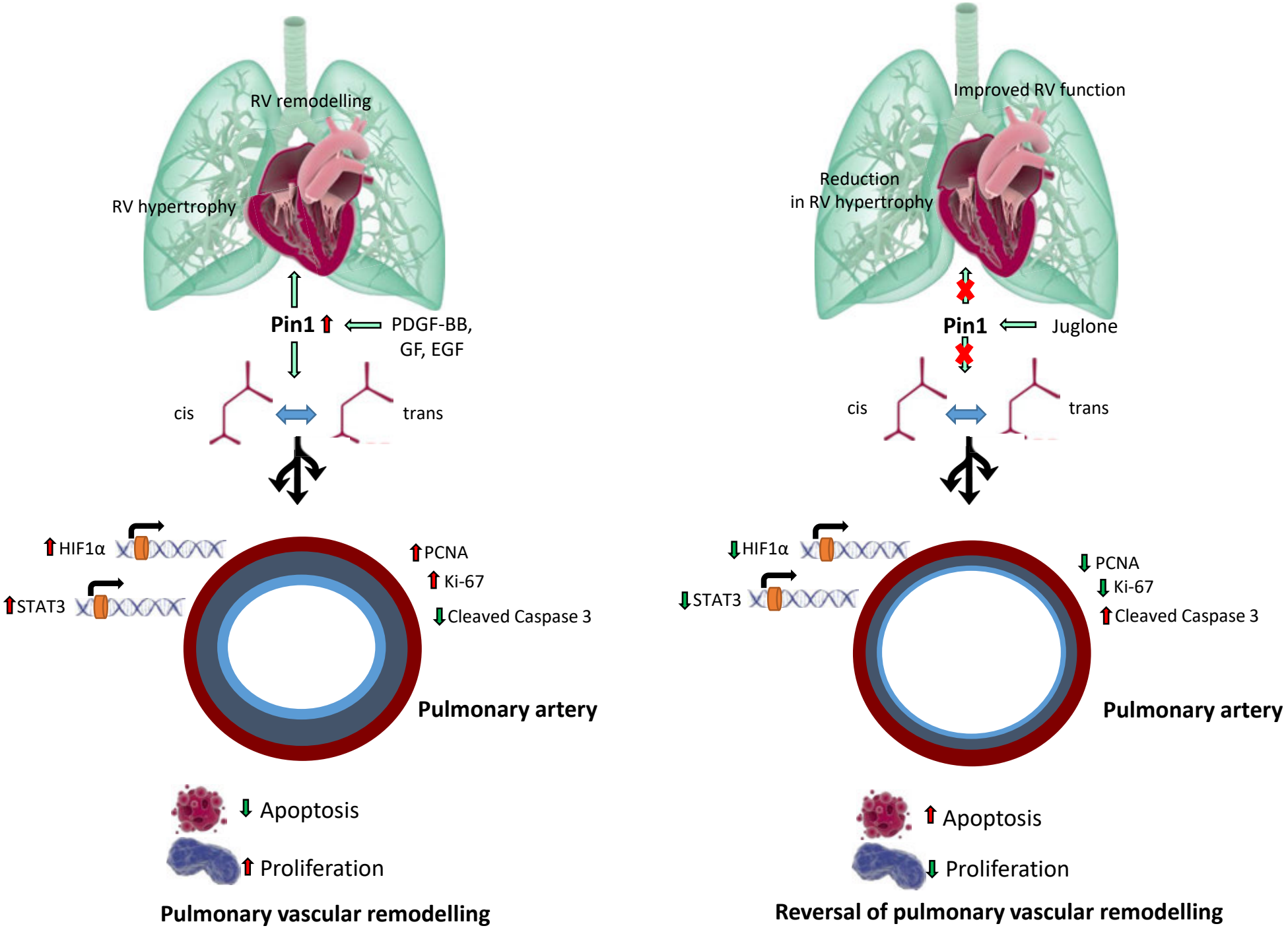
RV remodelling
RV hypertrophy
Pin1
PDGF-BB,
GF, EGF
cis
trans
HIF1α
STAT3
PCNA
Ki-67
Cleaved Caspase 3
Pulmonary artery
Apoptosis
Proliferation
Pulmonary vascular remodelling
Improved RV function
Reduction
in RV hypertrophy
Pin1
Juglone
cis
trans
HIF1α
STAT3
PCNA
Ki-67
Cleaved Caspase 3
Pulmonary artery
Apoptosis
Proliferation
Reversal of pulmonary vascular remodelling

Supplement Methods

Animals

All animal handling was performed complying with national and international directives as well as approved by the local authority Regierungspraesidium, Giessen, Germany (GI20/10 Nr. G82/2018). Adult male C57Bl6 mice (21–24 g body weight) and adult male Kyoto Wistar rats (200-250g), aged between 10-12 weeks, were obtained from Charles River Laboratories. All the animals were housed under controlled temperature (21–23°C), humidity (70%) and lighting (7AM-7PM light, 7PM-7AM dark) conditions and were fed a standard diet.

Human Pulmonary Arterial Smooth Muscle Cell (PASMC)

Human PASMCs from donor controls (n = 5) and patients with IPAH (n = 9) were obtained from Lonza (CC-2581, Basel, Switzerland) and UGLMC Giessen Biobank of the Justus-Liebig University Giessen (Giessen, Germany). The Ethics Committee of the Justus Liebig University has approved the biospecimen collection and isolation of primary cells of the UGMLC/DZL biobank according to the European IPS Registry (AZ 111/08) and the DZL Biobank (58/15). The patients have been informed and given their written consent for the use of biospecimen for research purposes. All studies and procedures to obtain human specimen were conducted according to the Declaration of Helsinki.

Primary hPASMCs were used between passages 5-8. Cells were cultured in Smooth Muscle Cell Growth Medium-2 (SmGM-2) with the supplement mix containing 5% fetal bovine serum, human fibroblast growth factor (2 ng/ml), human epidermal growth factor (0.5 ng/ml), and insulin (5 µg/ml) (PromoCell, Heidelberg, Germany). For proliferation analysis hPASMCs were starved in serum-free SMC Basal Medium (SmBM) without addition of supplements for 24 hours, followed by the treatment with varying concentrations of Juglone (1, 5, 10 µM) and stimulations with recombinant PDGF-BB (30 ng/ml; R&D Systems, Minneapolis, MN).

A table with a list of PH patients and control has been given below:

Table 1

IPAH

Nr.:	Age/Gender	Clinical Diagnosis	Final Diagnosis	Smoker	mPAP (mmHg)	PCWP (mmHg)	CI (l/min/m^2)	sPAP (mmHg)
221	39/F	PH	IPAH: severe PH. Ductus arteriosus		89	7	1.81	134
250	35/M	PPH / IPAH	IPAH		62	-	-	15
401	39/F	PAH / IPH	IPAH, pulmonary emphysema of medium size		-	-	-	-
449	34/F	PPH	IPAH		101	-	-	158
453	41/M	IPH	IPAH, mild chronic bronchitis, moderate pulmonary emphysema (Grade 4-5, according to Thurlbeck)		101	-	-	140
488	34/F	IPAH	IPAH, medium-sized blistered emphysema (Grade 4-5, according to Thurlbeck)		43	4	1.9	101
515	41/M	PPH	IPAH; Lung emphysema (Grade 4-5, according to Thurlbeck), plexiform lesions		48	15	3.1	130
GI-9	28/F	IPAH	IPAH		-	-	-	-
428	35/M	IPH	IPAH, lung emphysema (Grade 4-5)		62	10	2.2	80

Control (Biobank)

Nr.:	Age/Gender	Clinical Diagnosis	Final Diagnosis	Smoker
200	42/?	Donor	mild bronchitis, emphysema 3-4, moderate anthracosis, hypertensive vasculopathy 1-2	
553	30/M	Donor	Pulmonary emphysema grade 5-6 n.T., moderate chronic and active bronchitis, numerous condensate-containing alveolar macrophages, nicotine abuse?	
566		Donor	fibrosis	

Control (Lonza)

Nr.:	Age/Gender	Clinical Diagnosis	Final Diagnosis	Smoker
370750	51/M			No

Human Pulmonary Arterial Endothelial Cell (PAEC)

Control hPAECs were purchased from Lonza (Basel, Switzerland). IPAH-PAECs were obtained from Université Paris–Saclay, France. The human lungs used for IPAH-hPAEC cultures were obtained from patients with PAH during lung transplantation. Study patients were part of the French Network on Pulmonary Hypertension, a program approved by the institutional Ethics Committee, and had given written informed consent (Protocol N8CO–08–003, ID RCB: 2008-A00485-50, approved on June 18, 2008). PH was defined as resting mean pulmonary arterial pressure $\geqslant$25 mmHg. HPAECs were used between 3-5 passages. HPAECs were cultured in Endothelial Cell Growth Medium MV2 (Promocell, Germany). The supplement for growth medium includes fetal calf serum (0.05 ml/ml), recombinant human epidermal growth factor (5 ng/ml), recombinant human basic fibroblast growth factor (10 ng/ml), insulin-like growth factor (Long R3 IGF) (20 ng/ml), recombinant human vascular endothelial growth factor 165 (0.5 ng/ml), ascorbic acid (1µg/ml), hydrocortisone (0.2 µg/ml) as final concentrations.

Experimental PH model and treatments

Adult rats (control n=5, both placebo and Juglone treated n=10) were selected in a randomized manner and subcutaneously injected with the Sugen5416 (20 mg/kg body weight) solution in the neck. Immediately after the injection, animals were exposed to hypoxia (10% O_2) in the ventilated hypoxia chamber for three weeks, followed by re-exposure to normoxia for another two weeks. Control animals, injected with the same volume of saline, were kept in normoxic conditions for the same

duration. Adult mice (n=5 for control and placebo; n=10 for Juglone treated) were exposed to hypoxia (10% O_2) for three weeks, followed by two weeks of normoxia. Hemodynamic studies and tissue harvesting occurred at the end of the treatment. Mice and rats were subjected to intraperitoneal injection of Juglone with 3 mg/kg and 1.5 mg/kg per body weight every alternative day, respectively. Control mice and rats were injected with ethanol.

Echocardiography

Echocardiography was performed to measure several functional and morphometric measurements noninvasively, as described previously [1, 2]. The rats were anesthetized with isoflurane gas (3%) and the chest was shaved. Rats were kept in a supine position on a heating platform with limbs taped to ECG electrodes. Right ventricle internal diameter (RVID) was measured as the distance between the inner linings of the right ventricle free wall to the inner lining of the interventricular septum towards the right ventricle; it is measured in millimeters and serves as a parameter of right ventricle hypertrophy and dilatation. Stroke volume (SV) was measured as the volume of blood ejected by the ventricle during each contraction. Cardiac output (CO) was measured as the volume of blood ejected from the ventricle into the circulation per minute. Cardiac output equals SV multiplied by heart rate. Cardiac index (CI) was measured as the ratio of cardiac output per 100 grams of body mass; it estimates the performance of cardiac output according to the size of the body. Echocardiographic images were acquired with a VEVO 1100 (Visualsonics, Toronto, Canada) high-resolution imaging system equipped with MicroScan linear array transducers.

Assessment of pulmonary arterial hypertension

Mice were anesthetized with a subcutaneous injection of heparin (50 IU/kg body mass) to measure the hemodynamic parameters. A pressure catheter (SPR-671 Mikro-Tip®, Millar Instruments, Houston, Texas, USA) was inserted through the right jugular vein to measure right ventricular systolic pressure (RVSP), and into the left carotid artery to measure arterial pressure. The heart was dissected and weighed for calculation of the RV hypertrophy index (ratio of RV free wall weight over the sum of the septum plus LV free wall weight [RV/LV+S]).

Lung tissue harvest and preparation

Whole lungs were flushed through the pulmonary artery with saline. The right lobe was snap-frozen in liquid nitrogen and stored at -80ºC for molecular biology assessment, while the left lobe was perfused under 22 cm H_2O of pressure with 3.5 to 3.7% formalin, and immersed in formalin for 24 hours. Formalin-fixed lung tissue samples were stored in phosphate-buffered saline for 48 hours (changed after 24 hours) and dehydrated overnight. The lung tissues were then embedded and sectioned to 2µm thick sections on the fully automated rotation microtome (Leica, Wetzlar, Germany), and mounted on positively charged glass slides.

Assessment of medial wall thickness and occlusion of vessels

The assessment of medial wall thickness (MWT) and the occlusion score was performed with Elastica-van Gieson (EVG) staining. The percent medial thickness of muscular arteries (20-50µm) was calculated with the formula [(external diameter − internal diameter/external diameter) × 100] in EVG-stained slides. Next, the pulmonary vessels were categorized into open (≥75%), partially closed (75%-25%), and closed (<25%) in respect to the free area within the lamina elastic interna. Around 100 pulmonary vessels were analyzed at 630-fold magnification per lung section from each rat.

Laser-assisted micro-dissection of pulmonary vessels

Laser-assisted micro-dissection and pressure-catapulting technology (PALM Microlaser Technologies, Bernried/Germany) was performed at around 150 arteries (n = 6 for non-PAH control, n = 8 for IPAH) from each individual human. Each piece of micro-dissected tissue contained several cells. Each specimen was picked and processed for RT-PCR analysis. Methods of preparation, artery collection, total RNA extraction, and cDNA synthesis followed by quantitative real-time PCR analyses were as described in [3]. Before artery collection, cryosections from the lung, collected on glass slides were stained with Cresyl Violet for 4 min and Eosin Y for 20 s. Excessive dye was removed through rinsing slides with slow-running tap water for 1–2 min. RNeasy Mini kit (74106, Qiagen, Venlo, Netherlands) was used to isolate total RNA. In PCR experiments, the absence of any contaminating genomic DNA was validated by including reactions without RT during the first round of cDNA synthesis. Samples were also processed with no template controls (H_2O).

Western blot

Total protein extracts from cultured hPASMCs and hPAECs were isolated using cell lysis buffer (Thermo Fischer, Massachusetts, USA), and protein from lungs was isolated using the Cell Lysis Buffer (Cell Signaling Technology, Massachusetts, USA). Western blot analyses were performed with NuPAGE (NuPAGE™, Thermo Fisher Scientific, Massachusetts, USA) setup. Cell lysates were separated on a 4-12% SDS polyacrylamide gel (NP0336, NuPAGE™, Thermo Scientific, Massachusetts, USA) followed by transfer to a nitrocellulose membrane (#1620094, Bio-Rad, California, USA) of 0.45 µm thickness for 1 hour. The membrane was then blocked with 5% non-fat dry milk in Tris-Buffer Saline + 0.1% Tween 20 (TBS/T) for 45 minutes followed by overnight incubation with one of the following antibodies: Pin1 (sc-46660, Santa Cruz, Texas, USA), PCNA (sc-7907,Santa Cruz, Texas, USA), Cyclin D1 (sc-8396, Santa Cruz, Texas, USA), Cleaved-PARP (#9541, CST, Massachusetts, USA), PARP (#9532, CST, Massachusetts, USA), Caspase-3 (#9662, CST, Massachusetts, USA), HIF-1α (ab2185, Abcam, Cambridge, UK), C/EBP-α (sc-365318, Santa Cruz, Texas, USA), p-STAT3 (#9145, CST, Massachusetts, USA), STAT3 (#4904, CST, Massachusetts, USA) and Pan-actin (#4968, CST, Massachusetts, USA). Membranes were washed in TBS/T buffer, followed by incubation in secondary antibody coupled to horseradish-peroxidase and immunoreactive signals were detected by chemiluminescence reagent (RPN2232, ECL™ Prime, GE Healthcare, Buckinghamshire, UK). All the images were developed and analyzed on Amersham™ Imager 600 (GE Healthcare, Buckinghamshire, UK).

Reverse transcription-quantitative polymerase chain reaction (RT-qPCR)

The total RNA from the hPASMCs was isolated using the RNeasy Mini kit (74106, Qiagen, Venlo, Netherlands). The procedures were followed according to the manufacturer's instructions. The quality and concentration of total RNA were measured with a NanoDrop spectrophotometer (ND-1000, Peqlab, Erlangen, Germany). cDNA was generated by reverse transcription using M-MLV reverse transcriptase (M1302, Sigma, Munich, Germany) and oligo (dT) primer. The exon-spanning primer pairs for human, mouse, and rat genes were designed using the NCBI/ Primer-BLAST and are shown in Table 1. *HPRT* was used as the reference gene. Furthermore, qPCR was performed on a qPCR system machine (Mx3000P®, Stratagene, California, USA) using an iTaq™ SYBR® Green Supermix kit (#172-5124, Bio-Rad, California, USA), and procedures were followed according to manufacturer's instructions.

Table 2

Pin1	Homo sapiens	Fw 5'-GCAGCTCAGGCCGAGTGTA-3'
Pin1	Homo sapiens	Rev 3'-TGCGGAGGATGATGTGGATG-5'
Pin1	Mus musculus	Fw 5'-CACCCTACGCACCTTCCATT-3'
Pin1	Mus musculus	Rev 3'-GTTGAGGGGGCCTCTGTTAC-5'
Pin1	Rattus norwegicus	Fw 5'-AGCTCAGGCCGTGTCTACTA-3'
Pin1	Rattus norwegicus	Rev 3'-TGCTTTTCGCAACGGAACAG-5'
HPRT	Homo sapiens	Fw 5'-TGACACTGGCAAAACAATGCA-3'
HPRT	Homo sapiens	Rev 5'-GGTCCTTTTCACCAGCAAGCT-3'
HPRT	Mus musculus	Fw 5´-CAGTCCCAGCGTCGTGATTA-3´
HPRT	Mus musculus	Rev 5´-TGGCCTCCCATCTCCTTCAT-3´
HPRT	Rattus norwegicus	Fw 5'-ACAGGCCAGACTTTGTTGGAT-3'
HPRT	Rattus norwegicus	Rev 5'-GGCCACAGGACTAGAACGT-3'

si RNA transfections

PASMCs were serum-starved with Opti-MEM I medium (Fa. Gibco by Life Technologies, Carlsbad, California, USA) and then transfected with 30 nM of Pin1 (or control siRNA) lipoplexed with DharmaFECT1 (GE Dharmacon, Lafayette, Colorado, USA).

Transcription Factor Array

siRNA transfections with Pin1 siRNA or scrambled siRNA in hPASMCs were performed as described above. siRNA tranfections with Pin1 siRNA using Dharmacon ON-TARGETplusTM SMARTpool siRNA with 5'-CCACAUAACGCCAGC-3' sequence or scrambled-siRNA in hPAMSCs were performed. Similarly, hPASMCs were treated with either DMSO or Juglone (5 µM) and nuclear proteins were extracted with the nuclear extraction kit (#78833, NE-PER^{TM}, Thermo-Scientific, Massachusetts, USA). The nuclear extracts were incubated with biotin-labeled probe mix and TF-probe complexes were separated from free probes through a spin-column purification. The bound probes were detached from the complex and analyzed through hybridization with the 96-Well Plate. Complementary sequences of the probes are pre-coated in each well and the captured probe was further detected with Streptavidin-HRP Conjugate. A microplate luminometer (Infinite M200, TECAN, Männedorf, Switzerland) was used to detect luminescence (RLU).

Immunofluorescence staining

hPASMCs were cultured in a 24-well plate on a glass cover-slip. Serum starved cells were either treated with Pin1 siRNA or Juglone. The cells were then fixed with 3.7% paraformaldehyde (252549, Sigma-Aldrich, St. Louis, USA) and permeabilized with 0.5% Triton-X100 (T8787, Sigma-Aldrich, St. Louis, USA) . After incubating the cells in blocking buffer, mouse anti-Ki-67 (ACK-02, Leica Biosystems, Wetzlar Germany) was added and incubated overnight. The next day, cells were washed with 0.1% Nonidet P40 (74385, Fluka Biochemika, Buchs, Switzerland), and Alexa-flour goat anti-mouse (A11005, Life Technologies, California, USA) secondary antibody was added. After washing, the cells were stained with DAPI and visualized under fluorescence microscope BZ-9000 (Keyence, Japan).

Luciferase assay

hPASMCs were cultured in a 6-well plate. After serum starvation, siRNA transfections were performed using Pin1 siRNA, and cells were incubated for 24 hours. The next day, 9*HRE-luc reporter plasmid was overexpressed using Viromer® Yellow (lipocalyx GmbH, Halle, Germany) plasmid transfection reagent. A transfection complex with HRE reporter plasmid and Viromer® Yellow was prepared in supplemented buffer and given to the cells with fresh SmGM-2 medium. After 6 hours, the medium was replaced and the cells were kept in a hypoxia incubator (1% O_2) for 24 hours. Dual-Luciferase® Reporter Assay (E1960, Promega, Wisconsin, USA) was employed and manufacturer's instructions were followed to detect the HRE luciferase activity.

Mouse ventricular fibroblasts

Adult murine cardiac fibroblasts (CFs) were isolated from the right ventricle of mice. The tissue was washed with PBS and digested with the enzyme Liberase DH (cat. No. 05401089001, Roche, Mannheim). With various centrifugation steps, other cell types were separated and RVCFs were cultivated in DMEM medium (cat.no. E15-806, PAA, Cambridge, UK) with 10% FCS, 100 U/ml penicillin, and 10 µg/ml streptomycin. Early passage (1 or 2) CFs were used for all the experiments.

Collagen synthesis in cardiac fibroblasts

Serum starved CFs were treated with 5 µM Juglone and further stimulated with TGF-β1 (10 ng/ml) for 3 days. L-Ascorbic acid with an end concentration of 0.25 mM was added every day to the medium to stimulate collagen synthesis. Sircol Soluble

Collagen Assay (Biocolor Ltd, Carrickfergus, UK) was employed to detect the secreted collagen in the cell culture medium. Cold isolation & concentration reagent was added to each tube containing cell culture medium and incubated overnight at 0-4°C. The following day, the tube was centrifuged and the supernatant was removed carefully using cotton buds leaving a transparent pellet at the bottom. Sircol dye reagent was added and the concentration was determined using a spectrophotometer.

Assessment of right ventricular fibrosis

The RV tissue was freshly dissected and fixed overnight in 4% paraformaldehyde. After embedding in paraffin, the RV tissues were cut into 3 μm thin sections. To detect collagen fiber deposition in RV tissues, the Sirius Red assay (Sirius Red F3B, Bürstadt, Germany) with 0.1% Sirius Red in picric acid was applied. Leica Qwin V3 image analysis software (Leica Microsystem, Wetzlar, Germany) was used to analyze and quantify the amount of RV fibrosis.

Supplement Figure legends

Figure S1

Expression of Pin1 in human and experimental PAH

a) mRNA expression of *Pin1* in laser-assisted micro-dissected vessels (LMVs) from non-PAH controls and IPAH patients (control=6, IPAH=8). **b)**, **c)** mRNA analyses and protein expression of Pin1 in lung homogenates from control individuals and IPAH patients (control=5, IPAH=5). **d)** Protein expression of Pin1 in mouse smooth muscle cells (SMCs) exposed for 24 hours to 1% O_2. Data from four independent experiments are presented as mean ± SEM**. e)** & **f)** mRNA analysis of *Pin1* in lung homogenates from rats (NOX=5, SuHx=6) and mice (NOX=3, HOX=3) respectively, exposed to 10% O_2 for 3 weeks. *p<0.05. Statistical analysis was performed using Student's t-test.

Figure S2

Pin1 expression in PAH experimental animal models

Representative immunofluorescence images of lungs sections from **a)** Normoxia (NOX) vs. Sugen/Hypoxia (SuHx) rats and from **b)** Normoxia (NOX) vs. chronic-hypoxia (HOX) mice stained with Pin1 (green) and α–smooth muscle actin (α–SMA) (red). Scale bar: 50 μm.

Figure S3

Pin1 ablation affects the apoptotic resistance and proliferative capacity of human pulmonary vascular cells

a-c) Representative images of Ki-67 expression (red) upon Pin1 silencing or Juglone treatment in control and IPAH human pulmonary arterial smooth muscle cells (hPASMCs). **d-g)** Representative images of terminal deoxynucleotidyl transferase dUTP nick end labeling (TUNEL) of control and IPAH **d,e)** hPASMCs and **f,g)** human pulmonary arterial endothelial cells (hPAECs) upon Juglone treatment. Scale bar: 50 μm.

Figure S4

Analysis of Pin1 expression in human pulmonary arterial smooth muscle cells

a), b) Control human pulmonary arterial smooth muscle cells (hPASMCs) and **c), d)** IPAH hPASMCs, stimulated with Bone Morphogenetic Proteins (BMPs) and cytokines after 24h of serum starvation, subjected to enzyme-linked immunosorbent assay (ELISA) for Pin1 protein analysis. Data from two independent experiments are presented as mean ± SEM. **e)** Effect of Juglone administration on systemic systolic blood pressure (SBP, mmHg) in SuHx rats.

Figure S5

Effect of Juglone on Sugen/Hypoxia (SuHx) induced PAH in rats

a) Representative images of SuHx lung sections stained with von Willebrand (brown) and α–smooth muscle actin (purple) for the degree of muscularization. **b)**, **c)** Elastica van Gieson (EVG) staining on lung sections for medial wall thickness and occlusion of vessels and their respective representative images. **d)** Representative images of PCNA+ cells in vessels in SuHx lungs with hematoxylin/eosin, as counterstain. Scale bar: 50 µm. **e**) Representative images of Picrosirius red-stained right ventricular sections from NOX, SuHOX and SuHOX+Juglone treated rats. **f)**, **g)** Western blot analysis followed by densitometry of proteins from lung homogenates of SuHx rats (NOX=4, SuHx=4, SuHx+Juglone=4).

Figure S6

Effect of Juglone on chronic hypoxia-induced PH in mice

a) Representative images of immunohistological stainings of chronic hypoxia lung sections with von Willebrand Factor [vWF] (brown) and α–smooth muscle actin (purple) for the degree of muscularization. Scale bar: 50 µm. **b)** Representative images of Elastica van Gieson (EVG) staining of lung sections for medial wall thickness. Scale bar: 20 µm. **c)** Immunofluorescence images of TUNEL+ cells (red), and **d)** Ki-67+ cells (green) in vessels of chronic hypoxia mouse lung sections. Scale bar: 50 µm. **e)** Effect of Juglone administration on systemic systolic blood pressure (SBP, mmHg) in chronic hypoxia mice. **f**) Western Blot analysis followed by densitometry of lung protein homogenates from chronic hypoxia mice (NOX=5, HOX=5, HOX+Juglone=5).

References

1. Amirjanians, M., et al., *Chronic intratracheal application of the soluble guanylyl cyclase stimulator BAY 41-8543 ameliorates experimental pulmonary hypertension.* Oncotarget, 2017. **8**(18): p. 29613-29624.
2. Pak, O., et al., *Mitochondrial hyperpolarization in pulmonary vascular remodeling. Mitochondrial uncoupling protein deficiency as disease model.* Am J Respir Cell Mol Biol, 2013. **49**(3): p. 358-67.
3. Schermuly, R.T., et al., *Phosphodiesterase 1 upregulation in pulmonary arterial hypertension: target for reverse-remodeling therapy.* Circulation, 2007. **115**(17): p. 2331-9.

a. LMVs

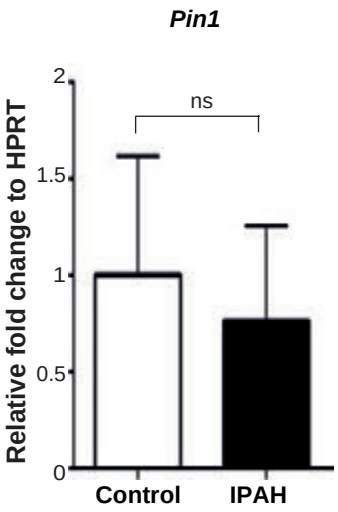

b. Human Lung

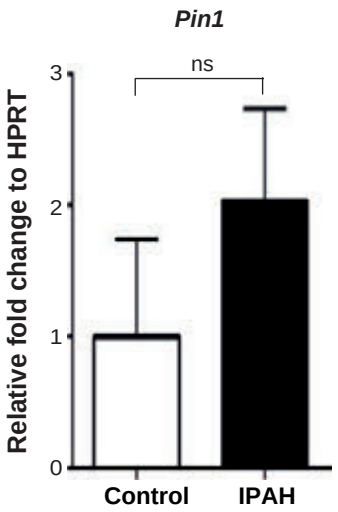

c. Human Lung

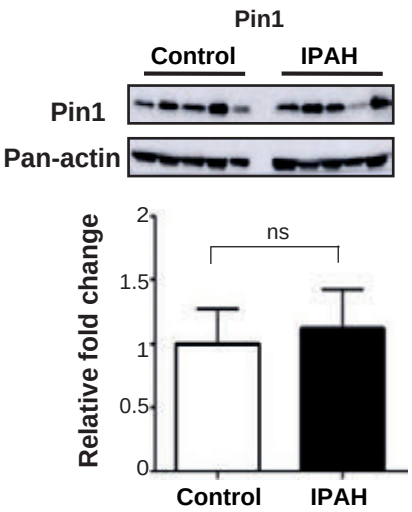

d. Mouse SMC

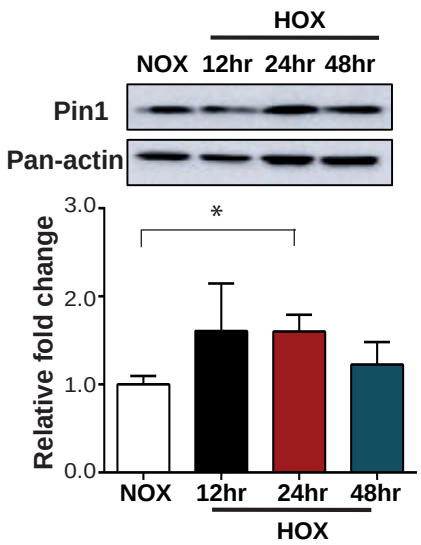

e. Rat Lung

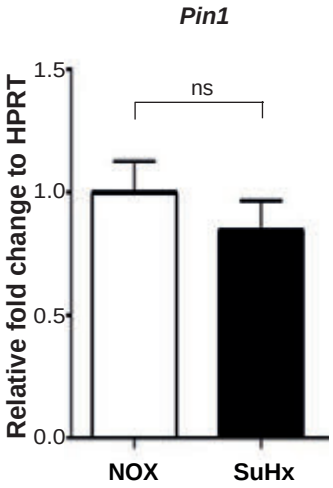

f. Mouse Lung

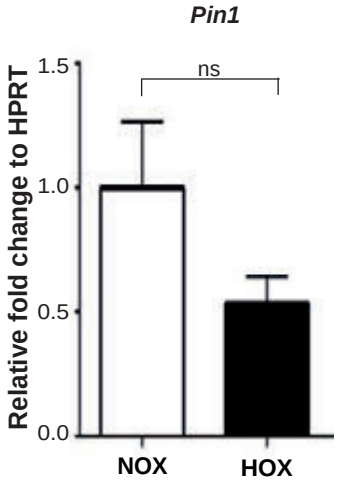

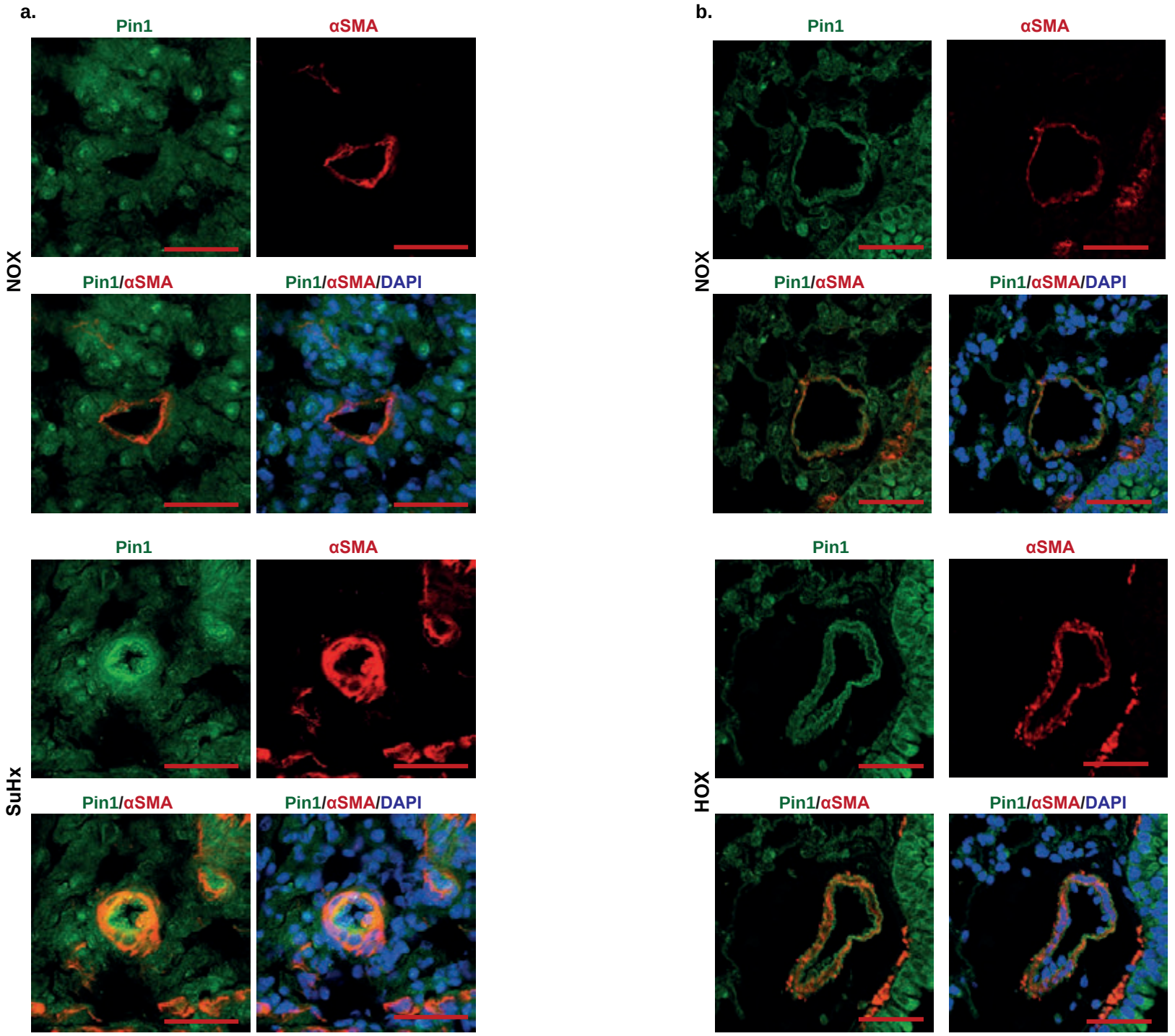
a.
Pin1
αSMA
NOX
Pin1/αSMA
Pin1/αSMA/DAPI
Pin1
αSMA
SuHx
Pin1/αSMA
Pin1/αSMA/DAPI
b.
Pin1
αSMA
NOX
Pin1/αSMA
Pin1/αSMA/DAPI
Pin1
αSMA
HOX
Pin1/αSMA
Pin1/αSMA/DAPI

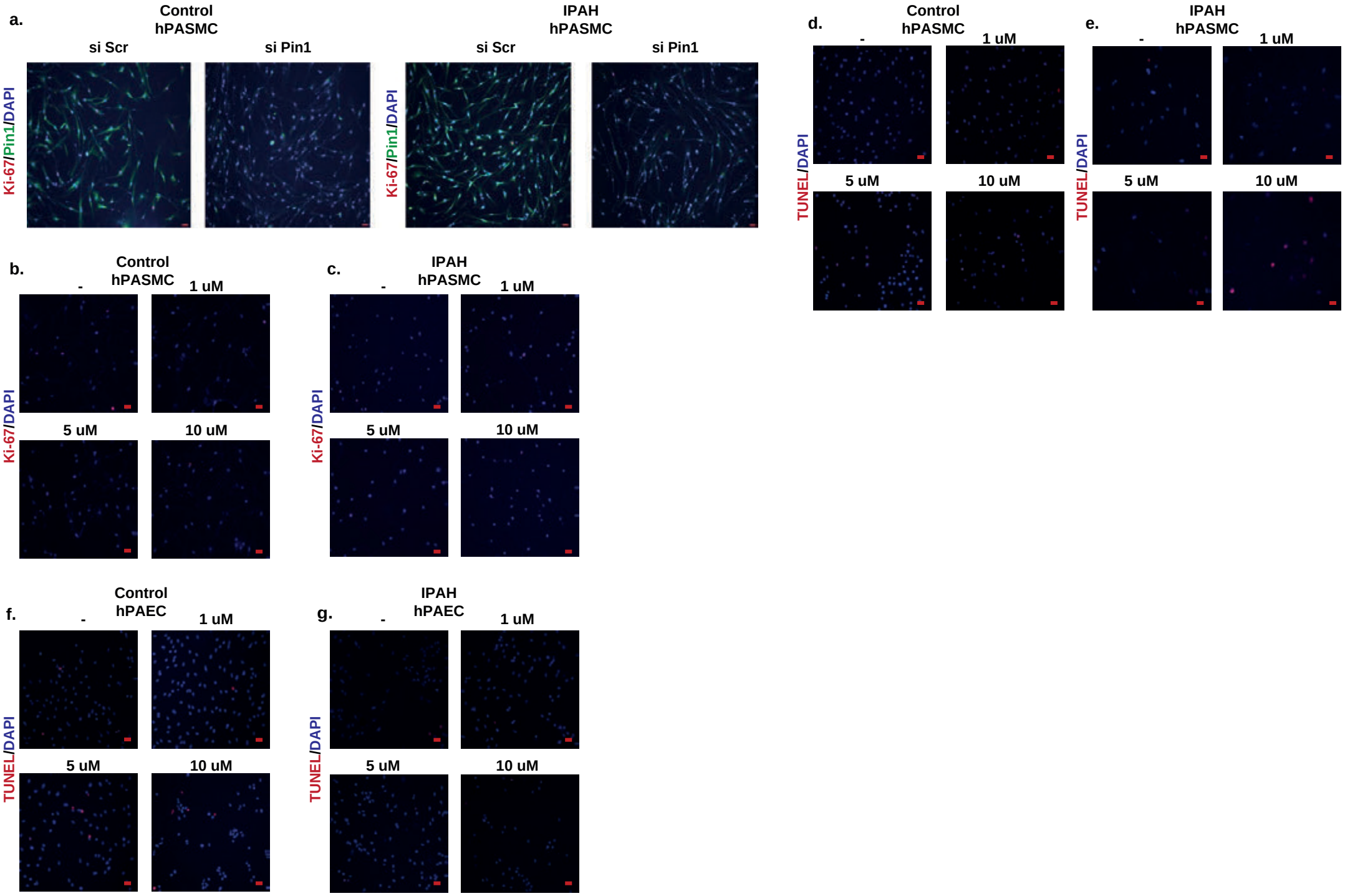
a.
Control hPASMC
si Scr
si Pin1
IPAH hPASMC
si Scr
si Pin1
Ki-67/Pin1/DAPI
b.
Control hPASMC
-
1 uM
5 uM
10 uM
Ki-67/DAPI
c.
IPAH hPASMC
-
1 uM
5 uM
10 uM
Ki-67/DAPI
d.
Control hPASMC
-
1 uM
5 uM
10 uM
TUNEL/DAPI
e.
IPAH hPASMC
-
1 uM
5 uM
10 uM
TUNEL/DAPI
f.
Control hPAEC
-
1 uM
5 uM
10 uM
TUNEL/DAPI
g.
IPAH hPAEC
-
1 uM
5 uM
10 uM
TUNEL/DAPI

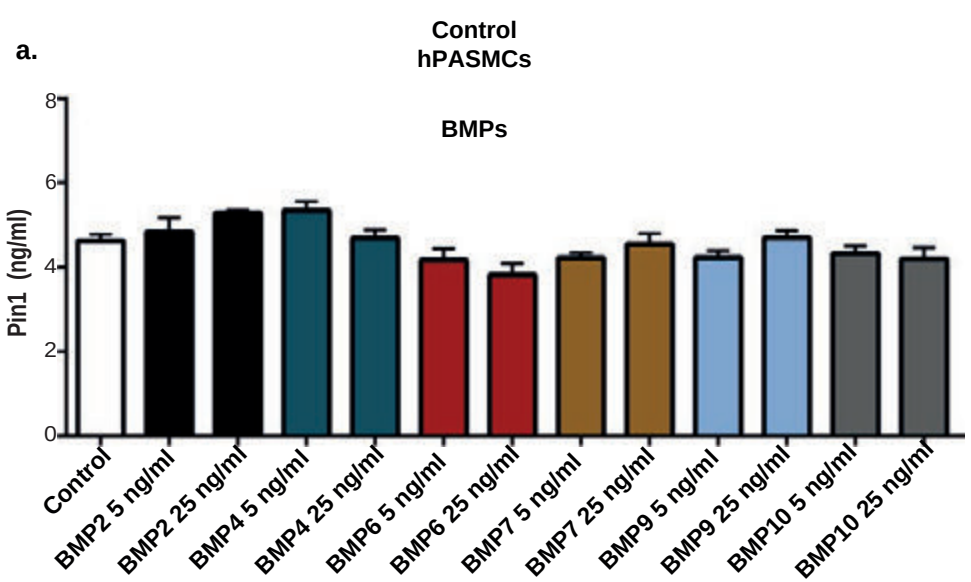
a.
Control
hPASMCs
BMPs
Pin1 (ng/ml)
0
2
4
6
8
Control
BMP2 5 ng/ml
BMP2 25 ng/ml
BMP4 5 ng/ml
BMP4 25 ng/ml
BMP6 5 ng/ml
BMP6 25 ng/ml
BMP7 5 ng/ml
BMP7 25 ng/ml
BMP9 5 ng/ml
BMP9 25 ng/ml
BMP10 5 ng/ml
BMP10 25 ng/ml

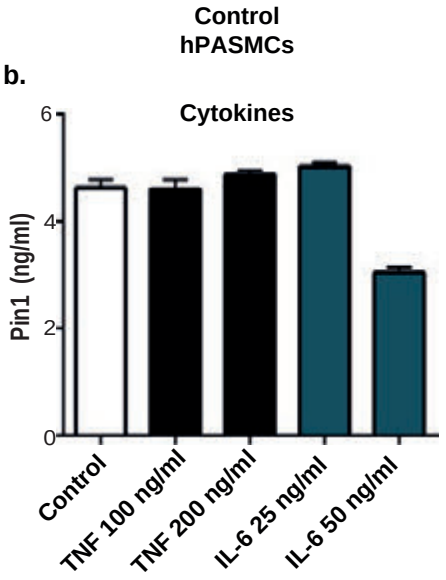
b.
Control
hPASMCs
Cytokines
Pin1 (ng/ml)
0
2
4
6
Control
TNF 100 ng/ml
TNF 200 ng/ml
IL-6 25 ng/ml
IL-6 50 ng/ml

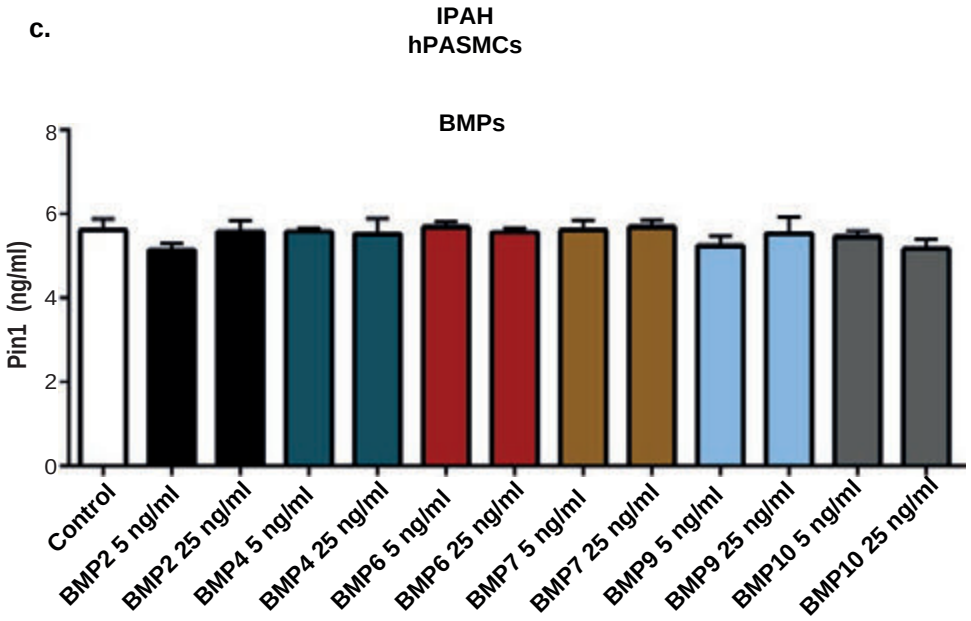
c.
IPAH
hPASMCs
BMPs
Pin1 (ng/ml)
0
2
4
6
8
Control
BMP2 5 ng/ml
BMP2 25 ng/ml
BMP4 5 ng/ml
BMP4 25 ng/ml
BMP6 5 ng/ml
BMP6 25 ng/ml
BMP7 5 ng/ml
BMP7 25 ng/ml
BMP9 5 ng/ml
BMP9 25 ng/ml
BMP10 5 ng/ml
BMP10 25 ng/ml

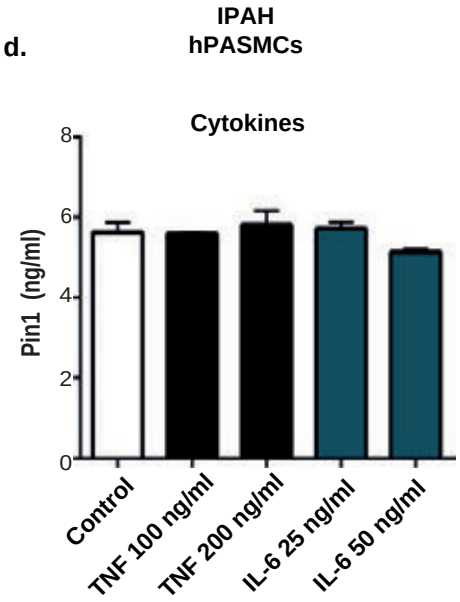
d.
IPAH
hPASMCs
Cytokines
Pin1 (ng/ml)
0
2
4
6
8
Control
TNF 100 ng/ml
TNF 200 ng/ml
IL-6 25 ng/ml
IL-6 50 ng/ml

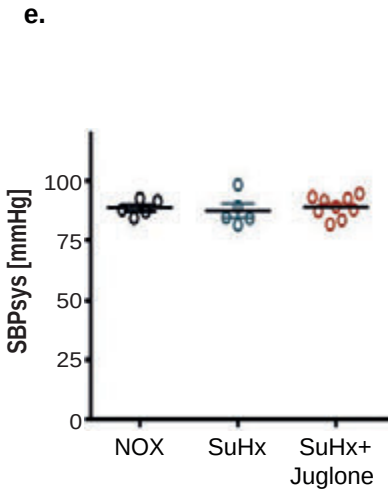
e.
SBPsys [mmHg]
0
25
50
75
100
NOX
SuHx
SuHx+
Juglone

a.

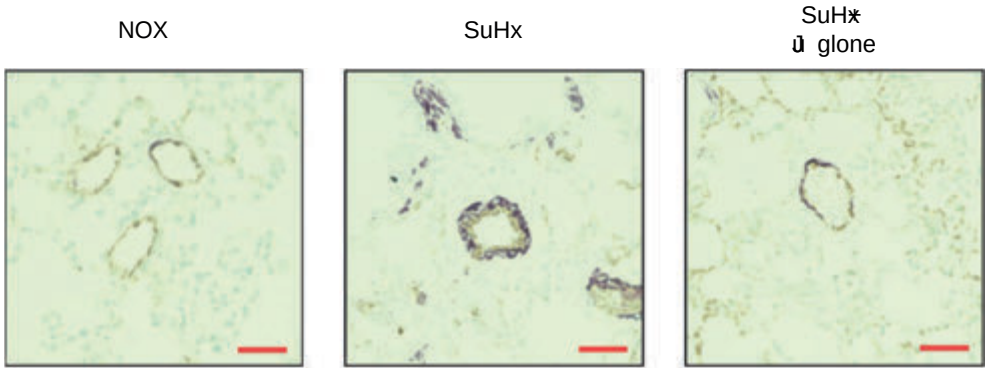
NOX
SuHx
SuHx + glone

b.

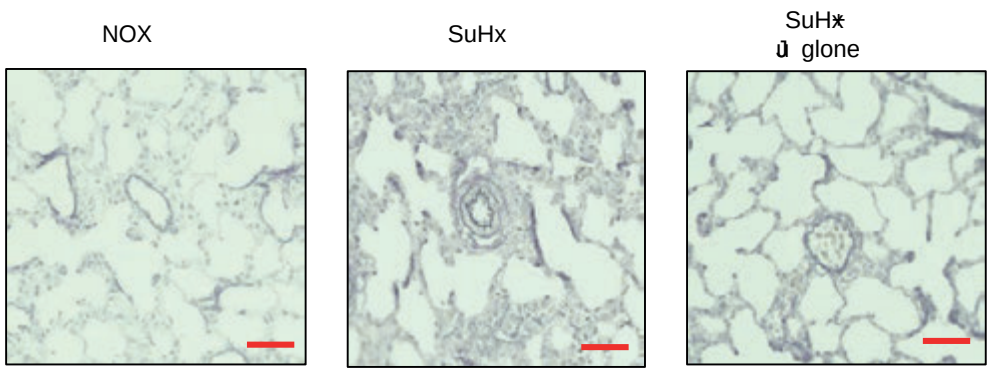
NOX
SuHx
SuHx + glone

c.

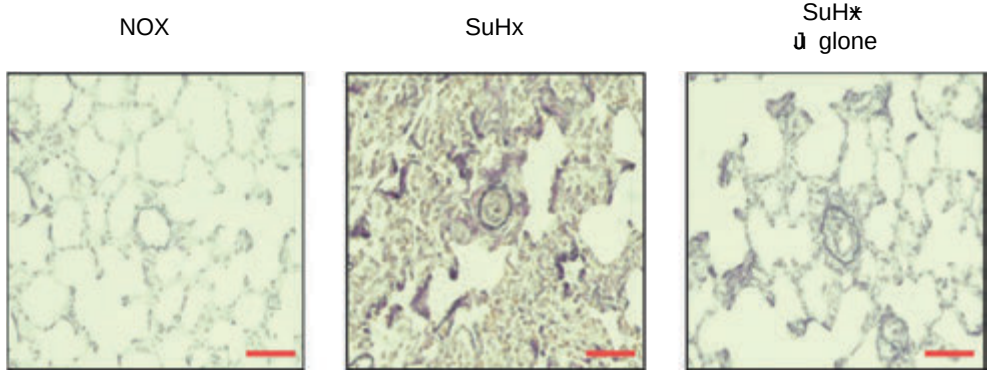
NOX
SuHx
SuHx + glone

d.

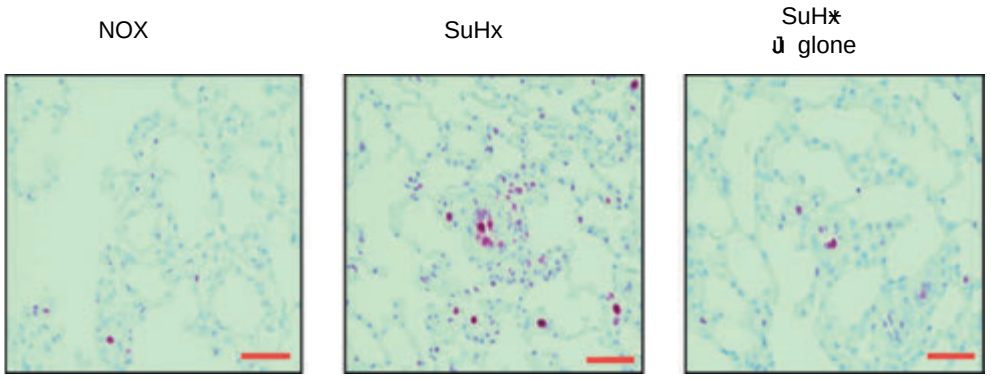
NOX
SuHx
SuHx + glone

e.


NOX
SuHx
SuHx + glone

f.

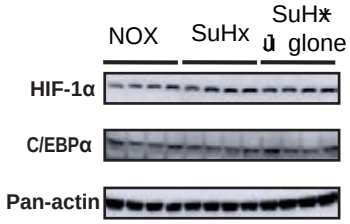
NOX
SuHx
SuHx + glone
HIF-1α
C/EBPα
Pan-actin

g.

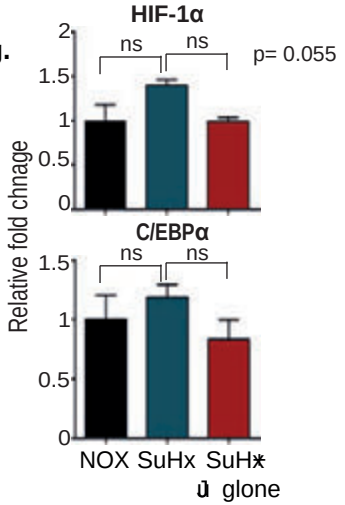
HIF-1α
ns
ns
p= 0.055
2
1.5
1
0.5
0
C/EBPα
ns
ns
1.5
1
0.5
0
Relative fold chnage
NOX
SuHx
SuHx + glone

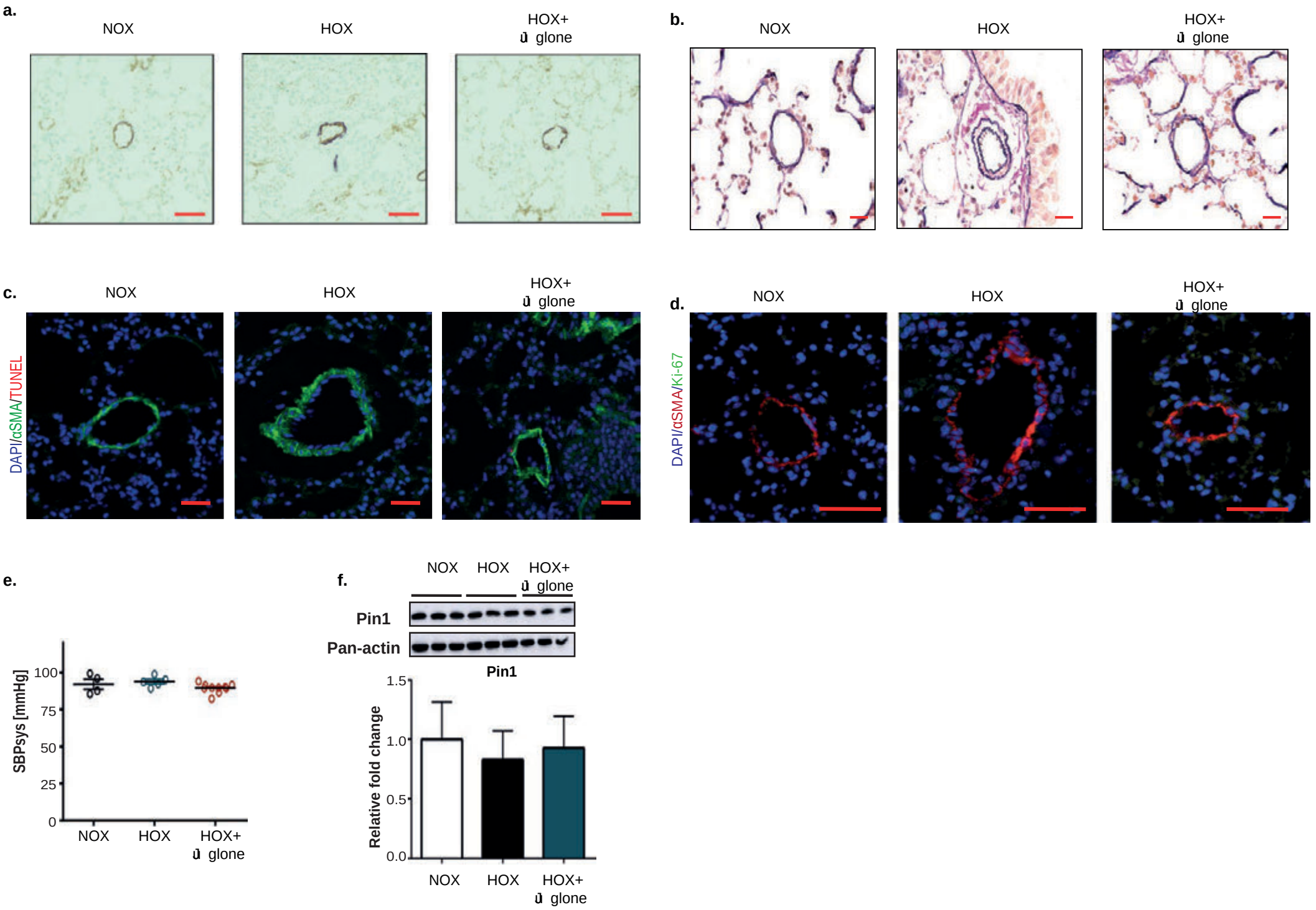
a.
NOX
HOX
HOX+
ů glone
b.
NOX
HOX
HOX+
ů glone
c.
NOX
HOX
HOX+
ů glone
DAPI/αSMA/TUNEL
d.
NOX
HOX
HOX+
ů glone
DAPI/αSMA/Ki-67
e.
SBPsys [mmHg]
100
75
50
25
0
NOX
HOX
HOX+
ů glone
f.
NOX
HOX
HOX+
ů glone
Pin1
Pan-actin
Pin1
Relative fold change
1.5
1.0
0.5
0.0
NOX
HOX
HOX+
ů glone